UNIVERSIDAD AUTÓNOMA DE SAN LUIS POTOSÍ

Postgraduate Degree in Interdisciplinary Sciences

Division of Biochemistry and Cell Biology

Analysis of pathogenic variants in retinoblastoma

Thesis presented by

Ana María Peña Balderas

To obtain the degree of

PhD in Interdisciplinary Sciences

Thesis co-directors:

Dr. Vanesa Olivares Illana

Dr. Jesús Hernández Monge

San Luis Potosí, S.L.P., August 2026

Certificate of thesis approval

The thesis **"Analysis of pathogenic variants in retinoblastoma,"** presented to obtain the degree of Doctor of Interdisciplinary Sciences, was prepared by Ana María Peña Balderas and approved on the august 2026 by the undersigned.

Dr. Vanesa Olivares Illana
Co-Director of the thesis

Dr. Jesús Hernández Monge
Co-Director of the thesis

_____
Advisor

_____
Advisor

_____
Advisor

Institutional credits

This thesis was elaborated at the Laboratory of Biomolecular Interactions and Cancer within the Biochemistry and Molecular Biology Line of the Interdisciplinary Sciences Graduate Program belonging to the Institute of Physics at the Universidad Autónoma de San Luis Potosí under the direction of Dr. Vanesa Olivares Illana and Dr. Jesús Hernández Monge.

During this work, the author received an academic scholarship from the Consejo Nacional de Humanidades Ciencia y Tecnología (No. 861707).

Life is not easy for any of us. But what of that?

We must have perseverance and above all confidence in ourselves

–Marie Curie

Dedication

To myself, for never giving up.
For moving forward through loss, change, pain, and hardship,
And for standing strong until I achieved my goal.
To me, who survived, fought, and won.

This thesis stands as a testament to my strength and perseverance.

Acknowledgments

To my thesis advisor, Dr. Vanesa Olivares Illana, for opening the doors of her laboratory to me for the second time, for her trust, perseverance, and patience, even in the most challenging moments.

To my thesis advisor, Dr. Jesús Hernández Monge, for being a great boss and, above all, a great friend. Thank you for sharing your knowledge, trusting me more than I trusted myself, listening to me, motivating me, and showing me that surviving a PhD is possible. It has been a privilege to work with you.

To my mother, Eloisa Balderas, for your infinite love, your unconditional support at every step of my life, and all the sacrifices that made this possible. Thank you for always believing in me. I love you!

To my boyfriend, Hugo Andrés Pérez Guerrero, for being by my side throughout this process, which has not been easy, and for never doubting my ability to achieve it. Thank you for your constant support, your words of encouragement, for always motivating me to keep going, and for your love.

To my brother José Orlando Peña Balderas, for always telling me, "¡Échale ganas!" and "¡Tú puedes!" and reminding me with humor that nothing is impossible.

To my dear friend and lab partner, Dr. Mayra Martínez Sánchez, for your support, your guidance, and everything I learned by your side. Thank you for the moments we shared, your sincere friendship, and for always inspiring me to be better.

To the academic technician, I.Q. Celina Gonzáles Gallegos from the Biomolecular Interactions and Cancer Laboratory, for your excellent work that makes mine possible, for always giving me a warm smile, for your unmatched charisma, and for the "¡Ánimos!" that was never lacking.

To all my friends for following this process, encouraging me, and always wishing me the best. Thank you for your support, laughter, affection, and for celebrating every achievement with me. You make the journey lighter and happier.

To the Consejo Nacional de Humanidades Ciencia y Tecnología (CONAHCyT) for the support provided through the scholarship No.861707.

Table of content

List of tables

List of figures

Abstract

Background. The RB protein encoded by the *RB1* gene is a tumor suppressor that regulates the cell cycle. Mutations in *RB1* are associated with several types of cancer; indeed, it was named after the first tumor suppressor linked to the development of retinoblastoma. This type of cancer is a pediatric ocular malignancy that originates from the retina. In 1971, Knudson proposed his two-hit hypothesis, which states that two mutational events are required to initiate tumor progression, sporadically or hereditarily. **Aims.** To characterize point mutations in the *RB1* gene associated with retinoblastoma, thereby contributing to the understanding of the molecular mechanisms underlying disease development. **Methods.** We analyzed four-point mutations in retinoblastoma, one synonymous mutation (pA14A), two missense mutations (pN328H and pD718N), and one with an early termination codon (pR552*), to characterize their cellular and molecular effects. We studied their mRNA and protein expression levels, proliferation, viability, localization, and migration using an RBKO cell line. **Results.** All mutants were expressed at the mRNA and protein levels. Regarding the subcellular localization of the mutants, pN328H was restricted to the nucleus, while pA14A, pR552*, and pD718N were present in both the nucleus and cytoplasm. The assays comparing the viability, proliferation, and migration of all variants versus wild-type RB showed significant alterations, particularly in mutant pR552*, which showed remarkable changes. The construct pR552* lacking the HA tag was generated. Once stably transfected, it was confirmed that the observed effects did not depend on the tag. Remarkably, the co-expression of both pR552* and wild-type RB showed that the pR552* mutant alone is sufficient to maintain the mutant phenotype. **Conclusions**. Our results suggest that the pR552* mutant exhibits gain-of-function (GOF) characteristics, as it not only loses its typical suppression function but also generates effects that alter cellular behavior.

Keywords: Retinoblastoma, *RB1,* point mutations, gain-of-function.

Resumen

Antecedentes. La proteína RB codificada por el gen *RB1*, es un supresor tumoral que regula el ciclo celular. Las mutaciones en *RB1* se asocian con diversos tipos de cáncer, de hecho, fue el primer gen supresor tumoral relacionado con el desarrollo de retinoblastoma. Este tipo de cáncer es una neoplasia maligna ocular pediátrica que se origina en la retina. En 1971 Knudson propuso la hipótesis de los dos golpes, la cual establece que se requieren dos eventos mutacionales para iniciar la progresión tumoral, ya sea de manera esporádica o hereditaria. **Objetivo** Caracterizar las mutaciones puntuales del gen *RB1* asociadas con el retinoblastoma, contribuyendo así a la comprensión de los mecanismos moleculares que subyacen al desarrollo de la enfermedad. **Métodos.** Se analizaron cuatro mutaciones puntuales en el gen *RB1* asociadas con retinoblastoma: una mutación sinónima (pA14A), dos mutaciones con cambio de sentido (pN328H y pD718N) y una mutación con codón de terminación prematuro (R552*), con el objetivo de caracterizar sus efectos celulares y moleculares. Se evaluaron los niveles de expresión de ARNm y proteína, así como la proliferación, viabilidad, localización subcelular y migración celular utilizando una línea celular RBKO. **Resultados**. Todas las mutantes se expresaron tanto a nivel de ARNm como de proteína. En cuanto a la localización subcelular la mutante pN328H se restringió al núcleo, mientras que pA14A, pR552* y pD718N se localizaron tanto en el núcleo como en el citoplasma. Los ensayos comparativos de viabilidad, proliferación y migración entre todas las variantes y la proteína RB de tipo silvestre mostraron alteraciones significativas, particularmente la mutante pR552*, la cual presento cambios mas notorios. Se generó una construcción de pR552* sin la etiqueta HA y tras su transfección estable, se confirmó que los efectos observados no dependían de dicha etiqueta. De manera destacada, la coexpresion de pR552* y RB silvestre demostró que la mutante pR552* por si sola es suficiente para mantener el fenotipo mutante. **Conclusiones.** Nuestros resultados sugieren que la mutante pR552* presenta características de ganancia de función, ya que no solo pierde su función supresora característica, sino que además adquiere propiedades que alteran el comportamiento celular.

Palabras Clave: Retinoblastoma, *RB1* mutaciones puntuales, ganancia de función.

1 Introduction

1.1 Mutations

A mutation is defined as a permanent alteration in the DNA sequence of an organism. Such changes may arise spontaneously during DNA replication or be induced by exposure to mutagenic agents, including chemical compounds, physical factors, or viral infections[1].

Depending on their biological consequences, mutations may have beneficial, neutral, or harmful effects on the organism, and in some cases they may even be lethal. Germline mutations are heritable because they occur in gametes, whereas somatic mutations arise in body cells and are not transmitted to offspring[1]. According to the level of genetic material affected, mutations are commonly classified as follows:

- Genetic or point mutations: These involve alterations affecting the nucleotide sequence of a single gene.
- Chromosomal: These involve structural rearrangements of chromosomes, including deletions, duplications, inversions, and translocations.
- Genomics: These cause variation in the number of chromosomes in a species, increasing the number of chromosome sets (polyploidy) or reducing it to a single set (haploidy or monoploidy), or affecting the number of chromosomes individually (by defect or excess).

1.1.1 Point Mutations

A point mutation consists of an alteration of a single nucleotide in the DNA sequence (adenine [A], guanine [G], cytosine [C], or thymine [T]) and may result from base substitution, insertion, or deletion.

Proteins are encoded by nucleotide triplets known as codons, each of which specifies a particular amino acid during translation. The genetic code consists of 64 codons generated

from combinations of the four mRNA nucleotides (A, G, C, and U). Of these, 61 encode amino acids, whereas the remaining three function as translation termination signals[2].

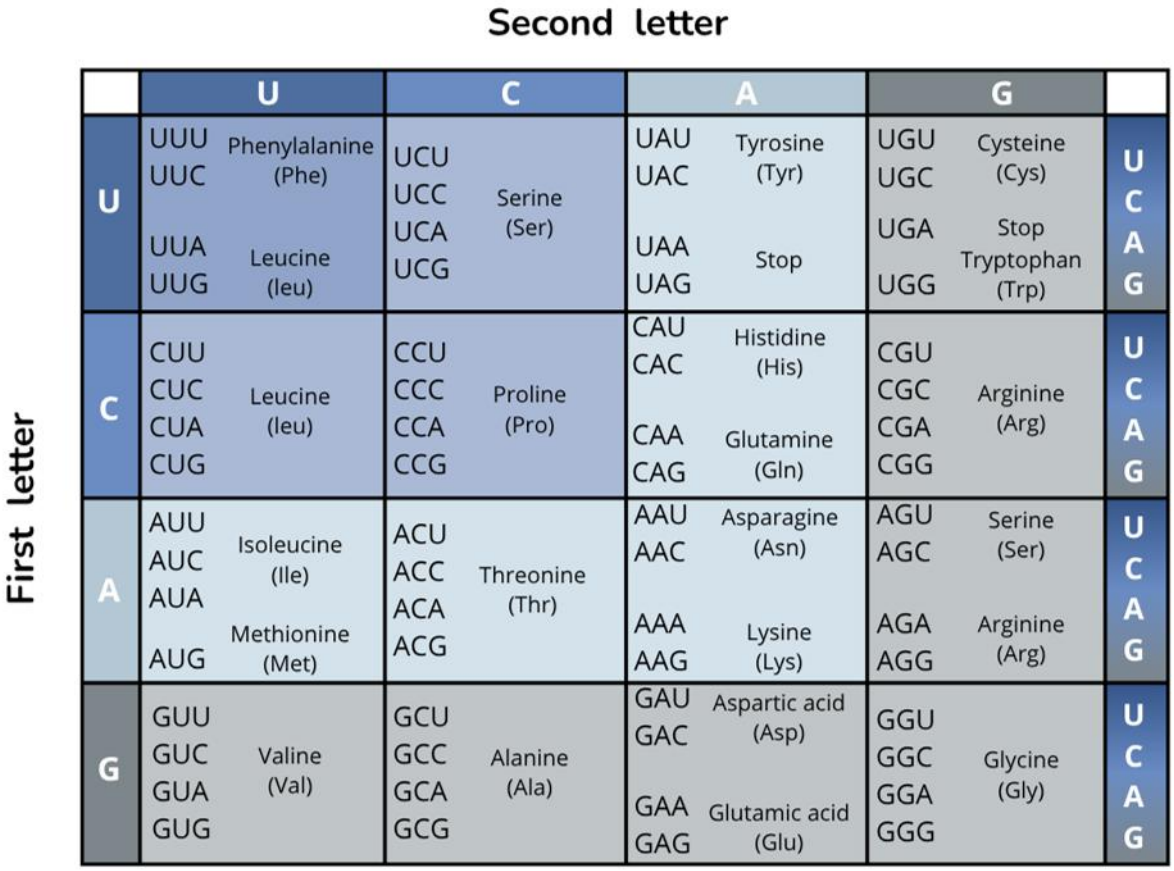

Figure 1.Standard genetic code.
Codons are composed of three mRNA nucleotides that specify individual amino acids or translation stop signals. AUG functions as the canonical initiation codon.

The biological consequences of point mutations depend on the codon involved. These variations can result in the synthesis of a protein with a different structure and function or the total absence of protein expression. We can classify the different types of gene mutations into[1,3]:

Base substitution mutations

A base substitution occurs when one nucleotide is replaced by another. At the DNA level, the replacement of a purine (adenine or guanine) with another purine, or of a pyrimidine (thymine or cytosine) with another pyrimidine, is referred to as a transition. In contrast, the

replacement of a purine with a pyrimidine, or vice versa, is defined as a transversion (Figure 2a). Based on their effects at the protein level, substitution mutations are classified as follows:

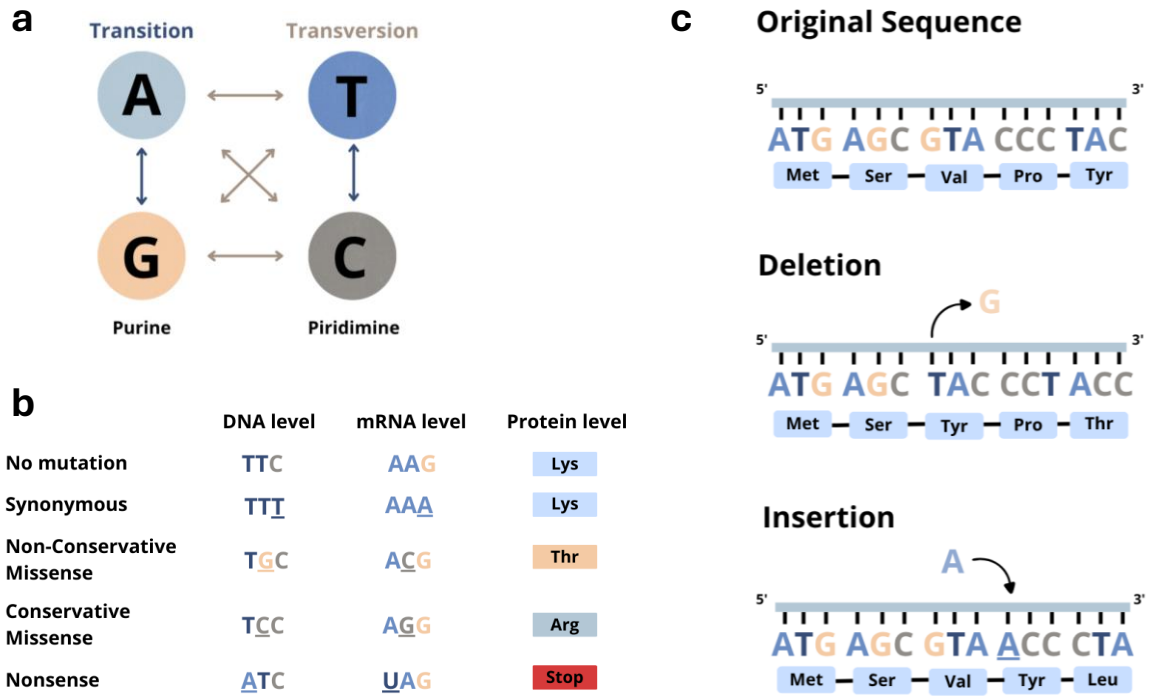

Figure 2. Classification of mutations.
a) Base substitution mutations can be classified into transitions (purine or pyrimidine to a pyrimidine) and transversions (purine to pyrimidine or vice versa) according to the type of nucleotide replacement. b) Depending on the effect on the codon and the resulting amino acid, substitution mutations can also be classified as: synonymous (they do not alter the amino acid), missense mutations (they change one amino acid for another), or nonsense mutations (they introduce a premature stop codon). Illustrative examples of each case are shown. c) The alteration of one or more nucleotides other than multiples of three, by deletion or insertion, causes a shift in the reading frame, which completely modifies the codon sequence from the site of the mutation.

- In **synonymous mutations**, a nucleotide change modifies the codon without altering the encoded amino acid (Figure 2b). This occurs because the genetic code is degenerate, and each amino acid has several combinations of triplets. Although synonymous mutations do not modify the amino acid sequence, they can still influence gene expression and protein function through multiple molecular mechanisms. These variants may alter pre-mRNA splicing, modify mRNA stability by changing its secondary structure, or create and disrupt miRNA-binding sites, thereby affecting transcript abundance. In addition, synonymous codons are not

translated with equal efficiency. Differences in codon usage, tRNA availability, and ribosome pausing can influence translation kinetics, which in turn affects co-translational protein folding and ultimately protein function[4,5]. Although synonymous variants were traditionally considered biologically silent, increasing evidence indicates that they contribute to numerous human diseases, including cancer. Approximately 20% of point mutations identified in tumors are synonymous, and an estimated 6-8% are thought to be under positive selection, suggesting that some may function as driver mutations, particularly in oncogenes[6].

- In **conservative missense mutations,** the altered codon specifies a different amino acid with similar physicochemical properties (Figure 2b). As a result, the protein often retains most or all its biological function[7].

- **Non-Conservative missense mutations** arise when a nucleotide substitution changes the encoded amino acid to one with markedly different physicochemical properties (Figure 2b). These substitutions are more likely to disrupt protein structure or function, frequently resulting in reduced or complete loss of biological activity[7].

- **Nonsense mutations** occur when the mutation results in a stop or termination codon (UAA, UAG, UGA). These cause the polypeptide chain to stop prematurely (Figure 2b), resulting in a truncated protein that, in many cases, lacks functionality or has altered activity[2,7]. Approximately 11% of the pathogenic variants causing inherited disorders correspond to nonsense mutations[8]. The effects of nonsense mutations can vary depending on the gene affected and the nature of the protein being produced. Some common effects include: **(a) mRNA degradation:** In some cases, truncated proteins are not formed because some organisms, including humans, use a degradation pathway for mRNAs containing nonsense mutations[9]. **(b) Loss-of-function (LOF):** Because the truncated protein is usually shorter than the original, it cannot perform its normal function in the cell. This type of LOF may be related to genetic diseases (such as cystic fibrosis and some forms of muscular dystrophy)[10]. **(c) Gain-of-function (GOF):** In some cases, the truncated protein can acquire new

aberrant functions such as promoting cell proliferation even in the presence of DNA damage, interfering with other tumor suppressor proteins, increasing resistance to apoptosis, or promoting migration, contributing to metastasis. An example of gain-of-function occurs in the tumor suppressor p53, where some nonsense mutations not only cause p53 to lose its ability to bind to DNA correctly, but also acquire the ability to interact with other transcription factors or proteins that promote tumor growth[11].

Reading frame shift mutations

Mutations caused by insertions or deletions of nucleotides that are not multiples of three alter the mRNA reading frame. As a result, the amino acid sequence is altered from the site of the mutation onward, often leading to the production of a truncated or non-functional protein[12] (Figure 2c).

1.2 Mutations and Cancer

A pathogenic variant is a genetic alteration that impairs the normal function of a gene and contributes to the development of disease. In cancer, the accumulation of pathogenic variants disrupts the molecular mechanisms responsible for maintaining normal cell growth, allowing cells to proliferate uncontrollably[13]. One of the fundamental concepts in cancer genetics is Knudson's two-hit hypothesis, first proposed in 1971. This hypothesis suggests that, for many tumor suppressor genes, both gene copies must lose their normal function before a normal cell can undergo malignant transformation. Consequently, two independent mutational events, referred to as hits, are generally required to initiate tumor development[14].

The mechanisms by which these two hits occur differ between hereditary and sporadic cancer. In hereditary cancers, individuals inherit one pathogenic variant in a tumor suppressor gene, meaning that only one additional somatic mutation is necessary to inactivate the remaining functional copy. In contrast, sporadic cancers develop when both mutational events are acquired independently during an individual's lifetime within the same cell[14].

The genes most frequently involved in cancer include tumor suppressor genes, proto-oncogenes, and DNA repair genes. Alterations affecting these genes interfere with essential

cellular processes such as cell cycle regulation, proliferation, apoptosis, and the maintenance of genomic stability, thereby promoting tumor initiation and progression[15].

A well-known example supporting the two-hit hypothesis is retinoblastoma, a rare pediatric malignancy caused by the loss-of-function of both alleles of the *RB1* tumor suppressor gene[15].

1.3 Retinoblastoma

Retinoblastoma is a rare malignant tumor that develops in the retina during early childhood and represents the most common primary intraocular cancer in children (Figure 3)[16,17]. The retina is a specialized light-sensitive tissue located at the back of the eye and is composed of several highly organized cell types, including photoreceptors (rods and cones), bipolar cells, horizontal cells, amacrine cells, ganglion cells, and Müller glial cells[16].

Current evidence suggests that retinoblastoma originates from cone photoreceptor precursor cells. Loss of *RB1* function disrupts normal cell cycle regulation, allowing these immature retinal cells to proliferate uncontrollably and ultimately give rise to tumor formation[16]. Because retinal development is still ongoing during the first years of life, retinoblastoma is diagnosed predominantly in children younger than five years old[17].

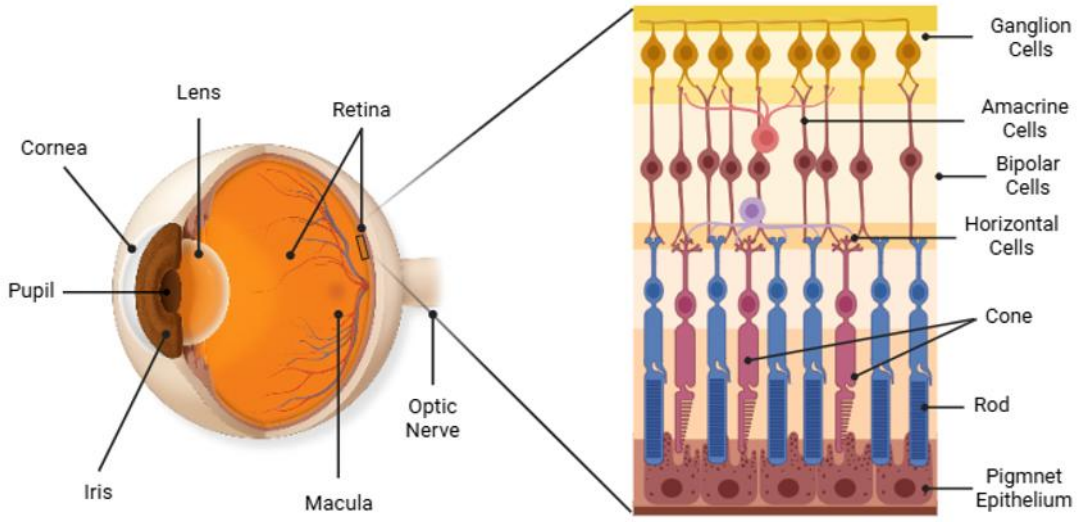

Figure 3. Cellular organization of the retina.
Illustration showing the principal retinal cell populations, including photoreceptors, bipolar, horizontal, amacrine, ganglion, and Müller cells, highlighting the layered organization involved in visual signal processing.

Retinoblastoma is the most common primary intraocular malignancy in children, accounting for approximately 3% of all pediatric cancer[18]. Its estimated global incidence ranges from 36 to 67 cases per million live births, with relatively little geographic variation[19]. Nevertheless, marked differences in survival exist between high- and low-income countries, largely because delayed diagnosis and limited access to specialized care remain major barriers to timely treatment[20].

In Mexico, the true incidence of retinoblastoma has not been fully established because a national registry is not available. Consequently, epidemiological information is derived primarily from referral centers and regional studies[19]. The General Hospital of the La Raza National Medical Center (IMSS), one of the country's main referral institutions, reports approximately 40.50 new cases annually, corresponding to an estimated prevalence of one case per 18,000 live births[19–21]. Despite survival rates exceeding 90% in high-income countries, the reported cure rate in Mexico is approximately 70%[19,20]. These disparities underscore the importance of early diagnosis and prompt access to specialized multidisciplinary care[22].

1.3.1 Diagnosis

Retinoblastoma is primarily diagnosed through clinical examination, based on characteristic signs such as leukocoria (white pupillary reflex), strabismus (ocular misalignment), hyphema (accumulation of blood in the anterior chamber), among other clinical manifestations (Figure 4)[23]. However, the appearance of these signs indicates significant progression of the disease.

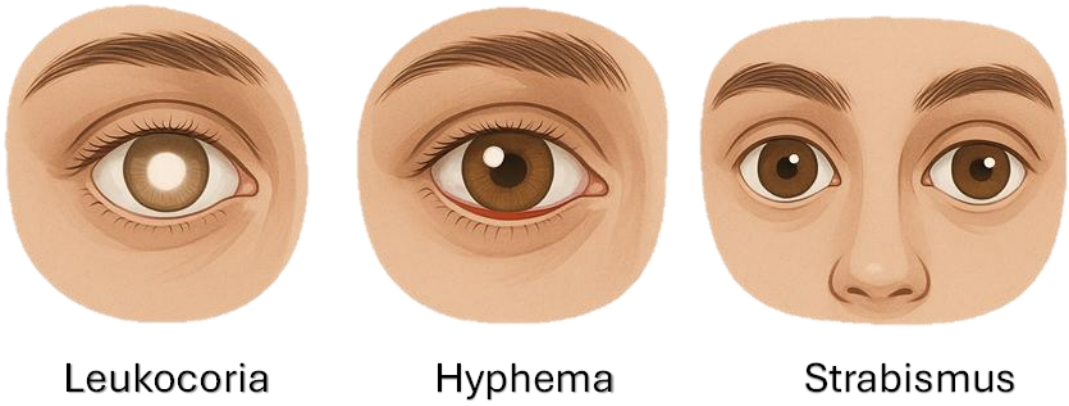

Figure 4. Signs associated with retinoblastoma.
Shown from left to right: leukocoria, hyphema, and strabismus. These clinical signs are common manifestations in patients with retinoblastoma, depending on the stage of the disease.

Accurate classification and staging are fundamental components of retinoblastoma management, as they provide essential information for prognosis and treatment planning. Although several staging systems have been proposed, none comprehensively incorporates all factors associated with disease risk at diagnosis. Among them, the International Classification for Intraocular Retinoblastoma (ICIR) has been widely validated and is considered a reliable predictor of treatment outcomes[19,24,25] (Table 1).

1.3.2 Treatment

The outcome of retinoblastoma treatment is strongly influenced by the timing of diagnosis, as early detection increases the likelihood of preserving both the eye and visual function. In many developing countries, delayed diagnosis results in a high proportion of patients presenting with advanced disease, making enucleation the most frequently performed treatment[21]. The therapeutic approach is selected according to several clinical factors,

including the patient's age, laterality, tumor size and location, extent of intraocular involvement, expected visual outcome, and overall systemic condition[18,26].

Table 1. Clinical characteristics of International Classification for Intraocular Retinoblastoma.

Groups	Characteristics
A	Small tumors (<3 mm) confined to the retina and located away from the fovea and optic disc.
B	Larger retinal tumors or lesions located close to critical structures, without vitreous or subretinal seeding.
C	Vitreous and/or subretinal seeding associated with discrete retinal tumors.
D	Diffuse vitreous or subretinal seeding with extensive intraocular tumor involvement, reducing the likelihood of globe salvage.
E	Eyes with advanced intraocular tumors and features associated with a poor visual prognosis or a high risk of extraocular extension; enucleation is generally recommended.

Depending on these characteristics, different treatment modalities may be used individually or in combination. Enucleation is generally reserved for eyes with extensive disease in which conservative treatment is unlikely to achieve adequate tumor control. Chemotherapy may be administered systemically or through targeted approaches, such as intra-arterial or intravitreal delivery, to reduce tumor burden and facilitate eye-preserving therapies. Local treatments, including cryotherapy, transpupillary thermotherapy, and laser photocoagulation, are primarily indicated for small tumors or as adjuvant therapies following chemotherapy. External beam radiotherapy, although less frequently used because of its long-term adverse effects, remains an alternative in selected patients when other therapeutic strategies are unsuccessful or contraindicated[18,26].

1.3.3 Clinical genetics

Several childhood malignancies are associated with alterations in a single gene. Retinoblastoma is a classic example, arising after the inactivation of both alleles of the *RB1* tumor suppressor gene[27]. This biallelic inactivation occurs in two distinct clinical forms: a hereditary form, which accounts for approximately 25% of cases, and a sporadic form,

representing the remaining 75%[27]. The development of these two forms is explained by Knudson's two-hit hypothesis, which states that both *RB1* alleles must be inactivated for tumor formation to occur[14]. In the hereditary form, which is commonly bilateral, one of the parents inherits a mutation to their offspring (first hit), so only one additional mutation (second hit) is needed for retinal cancer to develop. This form usually appears before 12 months of age (up to 5 years old), and the infant is more likely to develop other types of cancer in adulthood[28,29]. While the sporadic form is predominantly unilateral, parents pass on both healthy *RB1* alleles to their offspring. Mutations occur in each copy of the gene in the retinal cells, apparently at random, which eventually develop into a malignant tumor and manifest after 24 months[30] (Figure 5).

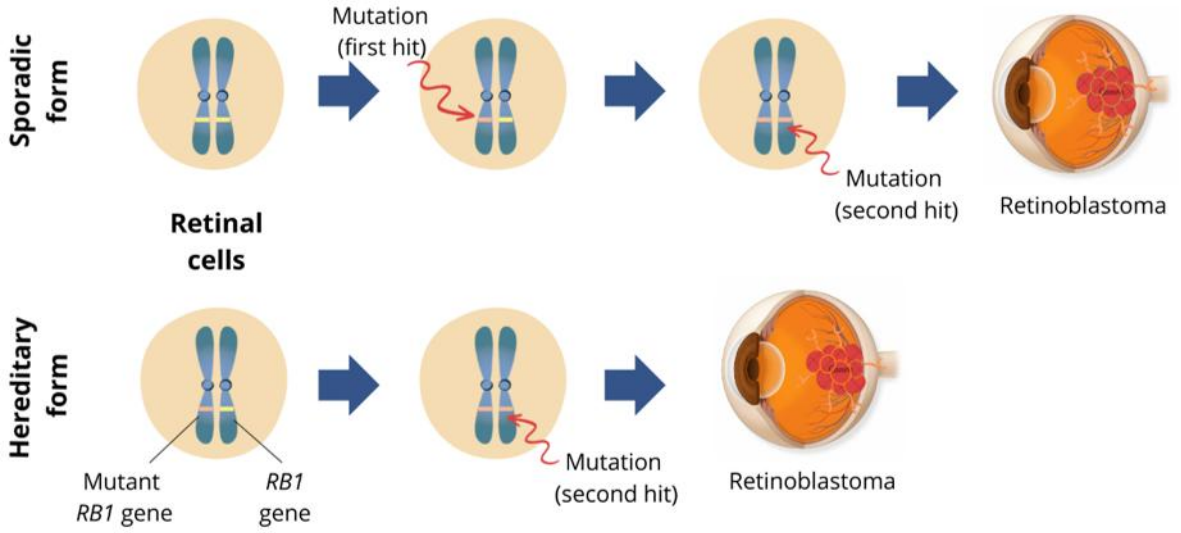

Figure 5. Schematic representation of the hereditary and sporadic forms of retinoblastoma according to Knudson's two-hit hypothesis.
In sporadic retinoblastoma (top), both *RB1* Gene activation events occur as somatic alterations within the same retinal cell, resulting in a later onset and typically unilateral disease. In hereditary retinoblastoma (bottom), the first *RB1* alteration is inherited through the germline and is therefore present in all cells, whereas the second event arises as a somatic alteration in the remaining functional allele, initiating tumor development.

1.4 RB

The retinoblastoma protein (RB) is a nuclear phosphoprotein encoded by the *RB1* gene, which is located on the long arm of chromosome 13 (13q14)[27]. RB belongs to the pocket protein family, together with p107 (RBL1) and p130 (RBL2). These proteins share a highly

conserved pocket domain that mediates interactions with viral oncoproteins as well as multiple cellular regulatory proteins, including members of the E2F family of transcription factors, thereby playing a central role in the regulation of cell-cycle progression[27,31].

The RB consists of 928 amino acids organized into three major structural domains. (Figure 6), an N-terminal domain of approximately 370 amino acids (RBN) involved in protein interactions, a central domain called RBAB consisting of an A domain and a B domain of 400 amino acids, required for most of the protein's functions, including cell cycle arrest, transcriptional repression, and chromatin structure regulation, and a C-terminal domain for approximately 140 amino acids (RBC) essential, together with the AB domain, for cell cycle arrest, for mediating RB regulation by phosphorylation, and for its degradation[32–34]. The N-terminal domain and the AB domain are each formed by a double cyclin motif, a folding motif common to the transcription factor TFIIB and cyclins[35,36], while the C-terminal domain has disordered structure in solution[37].

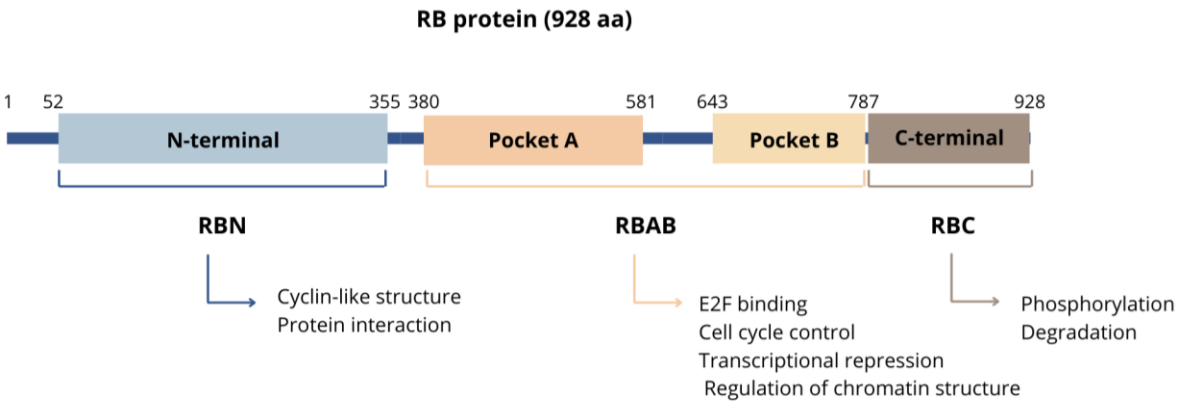

Figure 6. Schematic representation of the RB protein.
The protein is organized into three main structural domains: the N-terminal domain (RBN), the central pocket domain (RBAB), and the C-terminal domain (RBC), each one of which contributes to biological functions and different protein-to-protein interactions.

The tumor suppressor function of RB was initially uncovered through studies demonstrating its interaction with several viral oncoproteins, including adenovirus E1A, simian virus 40 (SV40) large T antigen, and human papillomavirus (HPV) E7[38–41]. These findings established RB as a central regulator of cell-cycle progression and provided the first evidence of its essential role in suppressing uncontrolled cellular proliferation[31].

The protein RB serves as a key regulator of the G1/S checkpoint, preventing the transition from the G1 phase to the DNA synthesis (S) phase and thereby controlling cell proliferation[32,42]. Its activity is regulated through reversible phosphorylation by cyclin-dependent kinases (CDKs). In its hypophosphorylated state, RB binds to members of the E2F family of transcription factors, repressing the expression of genes required for DNA replication and cell-cycle progression[31]. In response to proliferative signals, cyclins associate with CDKs to form active kinase complexes that phosphorylate and inactivate RB, resulting in the release of E2F transcription factors. This process promotes the transcription of genes required for entry into S phase, allowing cell-cycle progression[31,42] (Figure 7).

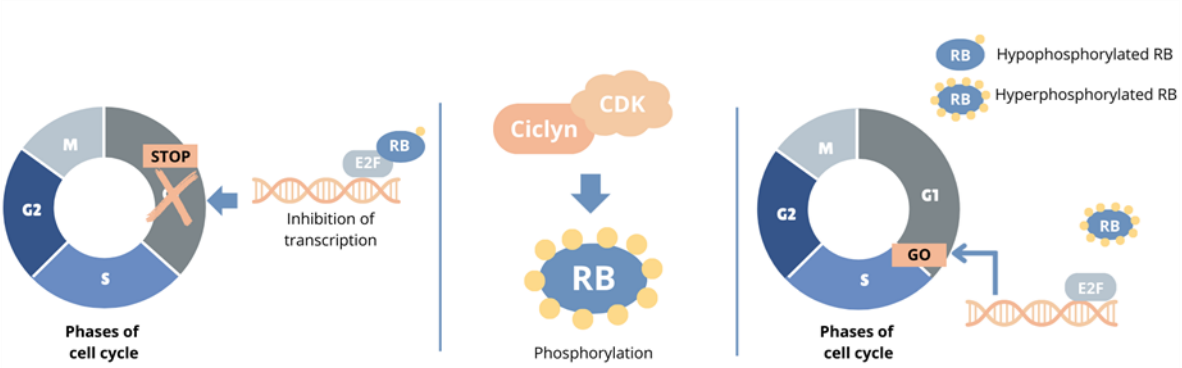

Figure 7. Function of the RB protein in the regulation of the cell cycle
In its hypophosphorylated state (active), the pRB binds to the transcription factors E2F, thus suppressing the expression of the necessary genes for the G1/S transition. After phosphorylation by cyclin-dependent kinases (CDK), the pRB inactivates itself functionally, releasing the transcription factor E2F and promoting the expression of genes implicated in DNA synthesis and the progression of the S phase.

The biological function of RB extends beyond the regulation of cell cycle progression. In addition to its canonical role as a tumor suppressor, RB participates in a wide range of cellular processes, including terminal cell differentiation[43,44], apoptotic processes in response to genotoxic damage[45], cell lineage specification during early development[46,] and chromatin structure regulation[31]. These functions described for RB are consistent with chromatin immunoprecipitation studies demonstrating its nuclear localization, and in particular, its association with chromosomes in regulatory complexes[47]. There are few studies on the degradation and regulation of RB, but it is known that several proteins are capable of

inducing RB via proteasomal degradation[48]. For example, the ubiquitin ligase proteins MDM2 and gankyrin[49,50].

Due to its essential role in cell regulation, the absence or abnormal forms of the protein can result in cell cycle dysregulation and subsequent unregulated cell proliferation.

1.5 RB Mutations

Most disease-causing variants affecting *RB1* correspond to loss-of-function alterations, including nonsense mutations. Frameshift variants, splice-site defects, and large genomic deletions. These genetic changes impair or abolish RB function, supporting the classification of *RB1* as a canonical tumor suppressor gene[51].

More than 3,000 mutations in *RB1* have been reported in the COSMIC (Catalogue of Somatic Mutations in Cancer) database[52]. This catalogue compiles mutations identified in human cancers; among these, more than 100 have been described in retinoblastoma (Figure 8). The reported variants include both base substitutions and frameshift mutations.

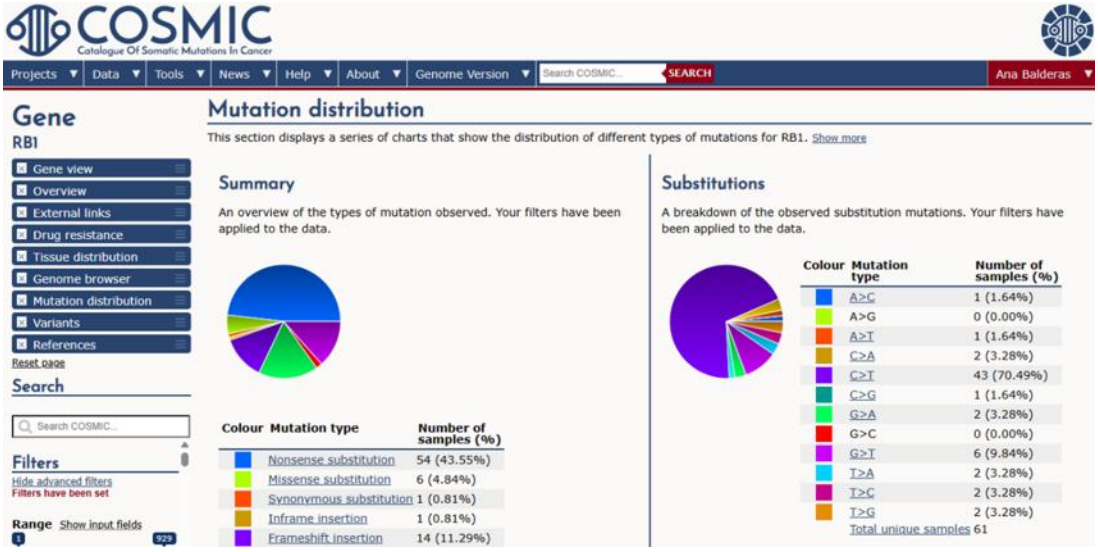

Figure 8. Distribution of RB1 gene mutations reported in the COSMIC database.
The portal summarizes the spectrum and frequency of somatic *RB1* variants identified across different human tissues and tumor types.

There are few studies of the effects of *RB1* mutations within the cell, despite the large number of mutations described to date. Therefore, the characterization of these variants is essential for understanding the molecular mechanisms underlying retinoblastoma development.

We selected some of the mutants mentioned above, a synonymous mutation pA14A, two missense mutations pN328H and pD718N, and a nonsense mutation pR552* to characterize their cellular effects. These mutations are located in different domains of the RB protein (Figure 9), and their characteristics can be seen in Table 2. Throughout this study, the resulting mutant forms of RB are collectively referred to as *RB1* variants.

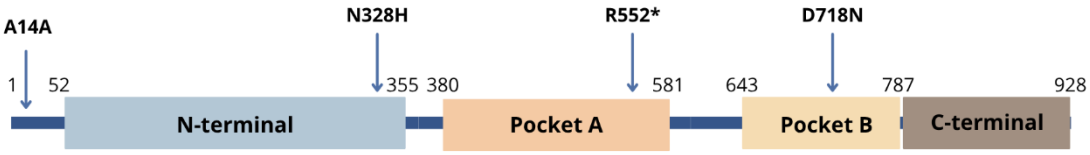

Figure 9. Representative diagram of the position of the mutant in the RB protein.
The position of a synonymous mutation (p.A14A), two missense mutations (p.N328H and p.D718N), and a nonsense mutation (P.R552*) are indicated. The mutations are distributed throughout key domains of the RB protein.

Table 2. Characteristics of RB mutants described in retinoblastoma

RB Mutants						
Position	**Mutation (Gene)**	**Mutation (Amino acid)**	**Type of Mutation**	**Primary tissue**	**Tissue Subtype 1**	**Histology**
14	c.42C>T	A14A	Synonymous mutation	Eye Skin	Retina NS	Retinoblastoma Carcinoma
328	c.982A>C	N328H	Amino acid change	Eye	Retina	Retinoblastoma
552	c.1654C>T	R552*	Stop codon	Eye Biliary tract Bone Breast Central nervous system	Retina Bile Duct NS NS Brain	Retinoblastoma Carcinoma Osteosarcoma Carcinoma Glioma
718	c.2152G>A	D718N	Amino acid change	Eye	Retina	Retinoblastoma

2 Materials and Methods

This chapter summarizes the experimental procedures performed in this study.

2.1 Cell cultures and generation of RB mutant cell lines

All experiments were performed using the human non-small cell lung carcinoma (NSCLC) cell line H1299. This cell line harbors a homozygous partial deletion of the *TP53* gene and therefore lacks expression of the p53 tumor suppressor protein. Since previous studies have demonstrated that loss of *RB1* induces p53-dependent apoptosis, the H1299 model provides an appropriate genetic background for studying RB function independently of p53. Based on this rationale, an H1299-derived cell line lacking RB expression (H1299 RB-/-) was generated and used throughout this study.

Cells were routinely maintained in culture medium supplemented with 10% fetal bovine serum (FBS), 2 mM L-glutamine, 100 U/mL penicillin, and 100 µg/mL streptomycin (Invitrogen), under standard cell culture conditions.

To evaluate the functional consequences of different RB variants, H1299 RB-/- cells were stably transduced with constructs encoding wild-type RB fused to a C-terminal hemagglutinin (HA) epitope tag (RB-HA), as well as the mutant proteins RBA14A, RBN328H, RBR552*, and RBD718N. Stable expression of each construct was achieved by antibiotic selection.

For plasmid construction, the full-length human *RB1* cDNA was cloned into the *HindIII* and *BamHI* restriction sites of the pcDNA3.1 vector (RRID: Addgene_14743). Before cloning, a sequence encoding the HA epitope was introduced at the C-terminal end of the RB protein to facilitate protein detection. The different RB mutants were subsequently generated by site-directed PCR mutagenesis using the RB-HA construct as the template.

Once confirmed, both the wild-type and mutant RB constructs were excised from the expression vector and subcloned into the retroviral vector pLNCX2 (RRID: Addgene_89818)

through the *HindIII* and *NotI* restriction sites. Purified plasmid DNA was used for retrovirus production in HEK293T cells (RRID: CVCL_0063) by transient co-transfection with plasmids encoding the viral packaging proteins Gag-Pol, which provide the capsid proteins, reverse transcriptase, and integrase, together with the VSV-G envelope glycoprotein. Transfections were performed using Lipofectamine 2000 according to the manufacturer's instructions.

Retroviral supernatants were harvested 48 hours after transfection and used to infect H1299 RB-/- cells in the presence of 8 μg/mL polybrene for 8 hours. Twenty-four hours after infection, cells were subjected to selection by supplementing the culture medium with G418 for a minimum of five days to obtain stable retrovirally transduced cell populations.

Additionally, the full-length human *RB1* cDNA was cloned into the *HindIII* and *BamHI* restriction sites of the c-Flag pcDNA3.1 vector for experiments requiring expression of Flag-tagged RB.

2.2 Generation of the H1299 RB-/- cell line

The H1299 RB-/- cell line was generated using the CRISPR/Cas9 genome-editing system (RRID: CVCL_0060). H1299 cells were co-transfected with the RB CRISPR/Cas9 knockout plasmid (cat. no. sc-400116, Santa Cruz Biotechnology, Santa Cruz, CA, USA), which encodes both the guide RNA targeting *RB1* and the Cas9 nuclease, together with the RB HDR plasmid (cat. no. sc-400116-HDR, Santa Cruz Biotechnology, Santa Cruz, CA, USA). This donor plasmid contains the homology-directed repair (HDR) template corresponding to the Cas9 cleavage sites, as well as a puromycin resistance cassette that enables the selection of successfully edited cells.

After transfection, stable knockout clones were isolated by serial dilution to obtain single-cell-derived colonies. Cells were maintained in culture medium supplemented with 3μg/mL puromycin (Sigma-Aldrich) to select for clones carrying the desired genomic modification.

To verify the successful disruption of *RB1*, individual clones were analyzed for RB protein expression by Western blot. Only those clones in which RB expression was undetectable were expanded and subsequently used for all downstream experiments.

2.3 Western blot analysis

To evaluate the expression of RB and its variants, total protein was extracted from cultured cells using radioimmunoprecipitation assay (RIPA) buffer containing 200 mM NaCl, 0.2% NP-40, 10% (v/v) glycerol, 1.0 mM dithiothreitol (DTT), 1.0 mM EDTA, and 25 mM Tris-HCl (pH 7.8). The lysis buffer was supplemented with 1% protease inhibitor cocktail (Cat. No. 4693132001, Sigma-Aldrich) to minimize protein degradation during sample preparation.

Protein concentration was then determined to ensure that equivalent amounts of total protein were loaded onto 8% sodium dodecyl sulfate-polyacrylamide gels (SDS-PAGE). The separated proteins were subsequently transferred to BioTrace NT nitrocellulose membranes (PALL Corporation) for immunodetection.

To reduce nonspecific antibody binding, membranes were blocked with 5% nonfat dry milk prepared in phosphate-buffered saline (PBS; pH 7.4). The membranes were subsequently incubated with the corresponding primary antibodies against RB (mouse anti-RB IF8; Cat. No. sc-102, Santa Cruz Biotechnology, CA, USA), HA (mouse anti-HA; Cat. No. ab130275, Abcam, USA), and β-actin (anti-actin-HRP; Cat. No. AC-15, Sigma-Aldrich). Finally, after the appropriate incubation and washing steps, protein expression was detected following standard immunoblotting procedures.

2.4 RNA extraction and quantitative real-time PCR (RT-qPCR)

To determine the expression levels of *RB1*, total RNA was first isolated from cultured cells using TRIzol reagent according to the manufacturer's instructions. Complementary DNA (cDNA) was subsequently synthesized from 1 μg of total RNA using M-MuLV reverse transcriptase (Cat. No. N01-M0253S, New England Biolabs).

Gene expression was then evaluated by quantitative real-time PCR (RT-qPCR) using SYBR Green chemistry. Amplification reactions were performed in triplicate with gene-specific primers targeting *RB1*, while *GAPDH* was used as the endogenous reference gene for normalization. The primer sequences were as follows: *GAPDH* forward, 5'-TCC AAA ATC AAG TGG GGC GA-3', and reverse, 5'-TGA TGA CCC TTT TGG CTC CC-3'; *RB1* forward, 5'-CCT CTC GTC AGG CTT GAG TTT-3', and reverse, 5'-GCT CTC TCT CTG ACA TGA TCT GG-3'.

Each reaction was prepared in a final volume of 10 µL containing cDNA template, gene-specific primers, and SYBR Green Master Mix (Thermo Fisher Scientific; Cat. No. K0221). Amplification was carried out in 96-well plates using a 7500 Fast Real-Time PCR System (Applied Biosystems).

The relative abundance of *RB1* transcripts was calculated using the comparative Ct ($2^{-\Delta\Delta Ct}$) method after normalization to *GAPDH* expression. This approach allowed the comparison of *RB1* mRNA levels among the different experimental conditions analyzed.

2.5 Immunofluorescence

To evaluate the subcellular localization of RB proteins in the different cell lines, immunofluorescence staining was performed. For this purpose, 3×10^4 cells were seeded onto sterile round glass coverslips placed in tissue culture-treated 24-well plates and incubated for 24 hours under standard culture conditions.

After the incubation period, cells were fixed with 3.7% paraformaldehyde for 30 minutes and permeabilized with 0.5% Triton X-100 in PBS for 1 hour. Cells were then washed with PBS and incubated in a blocking solution containing 3% bovine serum albumin (BSA) and 0.1% saponin for 30 minutes to reduce nonspecific antibody binding.

After blocking, cells were incubated overnight at 4°C with mouse anti-HA primary antibody (Cat. No. ab130275, Abcam, USA) diluted 1:100 in PBS containing BSA and

saponin. After washing with PBS, the samples were incubated with Alexa Fluor 568-conjugated anti-mouse secondary antibody (Cat. No. F0257, Sigma-Aldrich) diluted 1:1000. Finally, coverslips were mounted using a DAPI-containing mounting medium, and fluorescence images were acquired and processed using ZEN Lite 2012 software.

To further evaluate the intracellular localization of the RB p.R552* variant in the presence of wild-type RB, H1299 RB-/- cells were seeded at a density of 5×10^4 cells per well on sterile round glass coverslips placed in tissue culture-treated 24-well plates and allowed to adhere for 24 hours before co-transfection with RB-Flag and HApR552*. Cells were incubated for an additional 48 hours before fixation and permeabilization, following the same procedure described above.

After blocking, cells were incubated overnight at 4°C with a mixture of rabbit anti-HA antibody (Cat. No. ab236632, Abcam, USA) and mouse anti-Flag antibody (Cat. No. F1804, Sigma-Aldrich), both diluted 1:100 in PBS containing BSA. The cells were then incubated with Alexa Fluor 568-conjugated anti-mouse antibody (Cat. No. F0257, Sigma-Aldrich) and rhodamine-conjugated anti-rabbit antibody (Cat. No. ab6718, Abcam, USA) diluted 1:100 and 1:1000, respectively. Coverslips were then mounted using a DAPI-containing mounting medium, and fluorescence images were acquired and processed using ZEN Lite 2012 software.

2.6 MTT cell proliferation assay

To compare the proliferation rates among the different cell lines, cell viability was assessed using the MTT [3-(4,5-dimethylthiazol-2-yl)-2,5-diphenyltetrazolium bromide] colorimetric assay. This method estimates the number of viable cells based on their metabolic activity, as NADPH-dependent cellular oxidoreductase enzymes reduce the yellow tetrazolium salt (MTT) into insoluble purple formazan crystals. Consequently, the amount of formazan produced is directly proportional to the number of metabolically active cells.

For each cell line, 1×10^4 cells were seeded per well in 96-well plates containing 100µL of supplemented RPMI medium and incubated for 48 hours under standard culture conditions.

Following the incubation period, the MTT assay was performed using the MTT Assay Kit (Cell Proliferation; Cat. No. ab211091). The culture medium was replaced with serum-free medium containing the MTT reagent, allowing metabolically active cells to convert the tetrazolium salt into formazan crystals during a 3-hour incubation at 37°C. The resulting crystals were subsequently dissolved by adding the solubilization solution and incubating the plates for an additional 15 minutes at room temperature. Finally, absorbance was measured at 595 nm using a microplate reader, and the resulting values were used as an indirect measure of cell proliferation.

2.7 Colony formation assay

To evaluate the clonogenic capacity of the different cell lines, a colony formation assay was performed, which measures the ability of individual cells to survive, proliferate, and generate colonies over time.

For each experimental condition, 200 cells were seeded per well in 6-well plates containing 2 mL of supplemented RPMI medium and maintained under standard culture conditions for 10 days to allow colony formation.

At the end of the incubation period, cells were fixed with 100% methanol for 10 minutes at room temperature, followed by staining with 0.5% crystal violet solution for an additional 10 minutes to visualize the colonies. Excess dye was removed by washing the wells twice with double-distilled water (ddH_2O), and the plates were allowed to air dry before image acquisition. Colonies were photographed, and their number was quantified using the ColonyCount application.

2.8 Wound healing assay

Cell migration was evaluated using a wound healing assay to compare the migratory capacity of the different cell lines. To minimize the contribution of cell proliferation to wound closure, cells were treated with mitomycin C before the migration assay.

For each experimental condition, 7×10^4 cells were seeded per well in tissue culture-treated 24-well plates containing 500 µL of supplemented RPMI medium and incubated for 24 hours to allow the formation of a confluent monolayer. A linear scratch was then generated across the cell monolayer using a sterile pipette tip. Detached cells were removed by washing with 1× PBS, after which the cultures were incubated in serum-free medium containing 10µg/mL mitomycin C for 1 hour. Once the treatment was completed, cells were washed twice with 1× PBS and maintained in culture medium supplemented with 1% fetal bovine serum for the remainder of the experiment.

Images of the same microscopic field were acquired immediately after scratch generation (0 hours) and again at 24 and 48 hours to monitor wound closure over time. The percentage of wound closure was quantified using ZEN Lite 2012 software. The calculated closure rates were used to compare the migratory capacity of the different cell lines.

2.9 Statistical analysis

Unless otherwise indicated, all experiments were performed in at least three independent biological replicates, and each experiment included technical triplicates when appropriate. Data were analyzed using GraphPad Prism version 8.0 (RRID: SCR_002798) and are presented as the mean ± standard error of the mean (SEM).

Statistical differences among experimental groups were evaluated using one-way analysis of variance (ANOVA), followed by Bonferroni's multiple comparisons test when appropriate. Differences were considered statistically significant when the *p*-value was < 0.05. Statistical significance is indicated as follows: $*p < 0.05$, $**p < 0.01$, and $***p < 0.001$.

3 Results

3.1 H12299 RB-/- cell model

Before evaluating the functional consequences of the *RB1* variants, it was first necessary to establish a cellular model lacking endogenous RB expression. To accomplish this, the *RB1* gene was disrupted in H1299 cells, a non-small cell lung carcinoma cell line that lacks p53 expression, using CRISPR/Cas9-mediated gene editing.

Successful generation of the H1299 RB-/- cell line was first verified at the protein level by Western blot analysis. As shown in Figure 10a, endogenous RB protein was detected in the original H1299 cells but was absent in the H1299 RB-/- cell line, whereas RB expression was restored in cells stably expressing RB-HA. These findings confirmed the successful elimination of endogenous RB protein and the establishment of an RB-deficient cellular background.

To further validate gene disruption, *RB1* mRNA expression was quantified by RT-qPCR in H1299 wild-type and H1299 RB-/- cells. As expected, H1299 RB-/- cells exhibited a marked reduction in *RB1* transcript levels compared with wild-type cells (Figure 10b), providing additional evidence that CRISPR/Cas9-mediated editing effectively disrupted the *RB1* gene.

Together, these findings demonstrate that the H1299 RB-/- cell line provides a suitable experimental model for evaluating the biological effects of exogenously expressed RB variants. In addition, stable expression of RB-HA in this cellular background established the wild-type reference cell line used for comparison throughout the subsequent functional analyses.

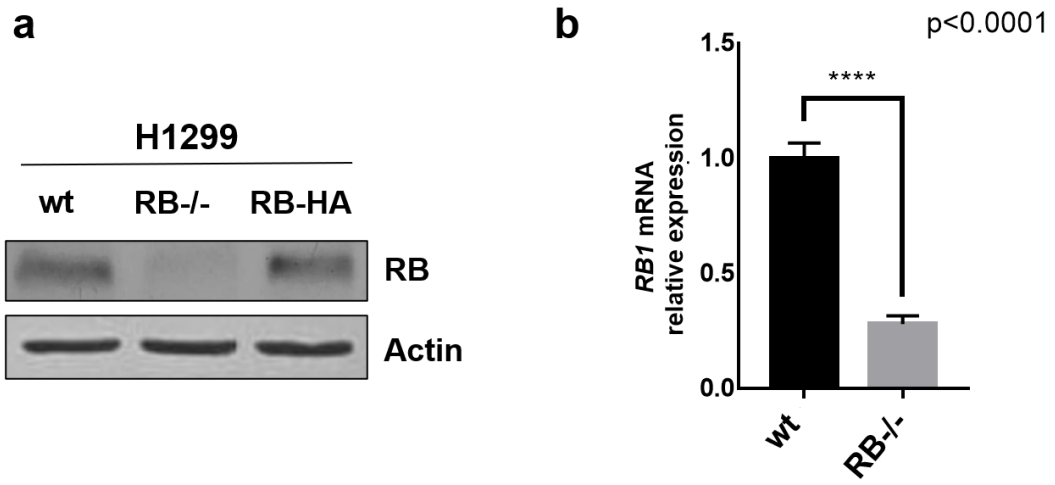

Figure 10. CRISPR/Cas9-mediated editing successfully disrupts *RB1* expression in H1299 cells. a) Western blot analysis demonstrates endogenous RB protein expression in H1299 wild-type cells, the absence of RB in H1299 RB-/- cells, and restoration of RB expression in H1299 RB-/- cells stably expressing RB-HA. b) RT-qPCR analysis reveals a significant reduction in *RB1* mRNA levels in H1299 RB-/- cells compared with H1299 wild-type cells. Results are expressed as mean ± standard deviation (SD). (****p<0.0001).

3.2 Expression and localization of *RB1* variants

Following the establishment of the H1299 RB-/- cell model, stable cell lines expressing each of the four *RB1* variants —A14A, N328H, R552*, and D718N— were generated by retroviral transduction of H1299 RB-/- cells with the corresponding HA-tagged constructs followed by G418 selection. This previously established cell line stably expressing wild-type RB-HA was used as the reference control. Before evaluating the biological effects of the variants, their expression was examined at the mRNA and protein levels, followed by analysis of their subcellular localization by immunofluorescence.

RT-qPCR analysis demonstrated that all four *RB1* variants were successfully transcribed in H1299 RB-/- cells, although their expression levels differed among the constructs. Compared with RB-HA, the HA-D718N variant showed comparable mRNA expression, whereas HA-N328H exhibited significantly lower *RB1* mRNA expression (Figure 11). These findings confirmed the successful transcription of all recombinant constructs.

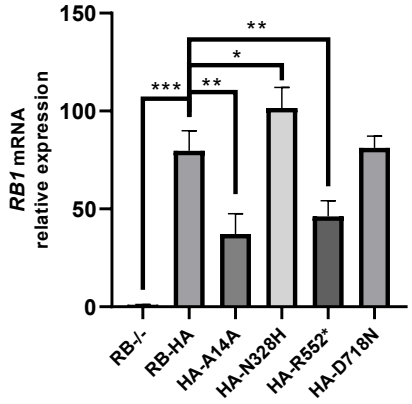

Figure 11. *RB1* variants exhibit differential mRNA expression in H1299 RB-/- cells.
RT-qPCR analysis shows differences in transcript abundance among the four *RB1* variants. Transcript levels were compared with those of H1299 RB-/- cells and cells expressing wild-type RB (RB-HA). Results are expressed as mean ± SD of three independent biological replicates. Statistical significance was determined by one-way ANOVA followed by Bonferroni's multiple-comparisons test (*p<0.05, **p<0.01, ***p<0.001, ****p<0.0001).

Protein expression was subsequently evaluated by Western blot analysis. An anti-RB antibody detected expression of the RB-HA control as well as the HApA14A and HApD718H variants. However, the HApN328H and HApR552* variants were not detected with anti-RB antibody. Since all constructs contained an HA tag, an anti-HA antibody was used to verify their expression. Anti-HA immunoblotting confirmed the expression of both the HApN328H and HApR552* variants, indicating that these proteins were expressed despite not being detected with anti-RB antibody. As expected, the HApR552* variant migrated at lower molecular weight than full-length RB, consistent with the production of a truncated protein resulting from the premature stop codon. β-actin was used as a loading control (Figure 12). Despite these differences, all mutant proteins were successfully detected, confirming expression of the recombinant constructs.

To determine whether the *RB1* variants retained their normal intracellular localization, immunofluorescence analyses were performed. As expected, RB-HA exhibited a predominantly nuclear localization pattern. Similarly, the HApN328H variant remained primarily localized in the nucleus (Figure 13), although the nuclei of these cells appeared smaller than those observed in RB-HA-expressing cells (Figure 14). In contrast, the HApA14A, HApR552*, and HApD718N variants displayed both nuclear and cytoplasmic

localization, indicating an altered intracellular distribution compared with the wild-type protein (Figure 13). During the immunofluorescence analysis, the nuclei of some *RB1* variant-expressing cells appeared smaller than those of RB-HA-expressing cells. To quantitatively assess this observation, nuclear area was measured from the DAPI-stained images. This analysis showed that both the HApA14A and HApN328H variants exhibited a significant reduction in nuclear area compared with RB-HA, whereas HApR552* and HApD718N maintained nuclear areas comparable to those of RB-HA (Figure 14).

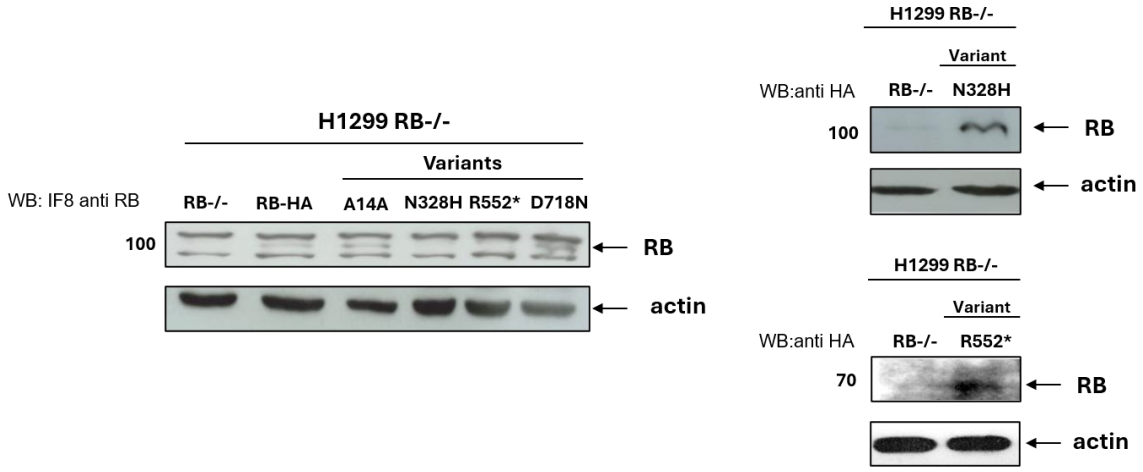

Figure 12. Expression of all RB variants is confirmed in H1299 RB-/- cells by Western blot analysis.
The RB protein variants (HApA14A, HApN328H, HApR552* y HApD718N) and the wild-type RB-HA protein were validated by Western blot. RB-HA and the HApA14A and HApD718N variants were detected using an anti-RB antibody (left panel), whereas the HApN328H and HApR552* variants were detected using an anti-HA antibody (right panel). β-actin was used as a loading control.

Together, these results demonstrate that all variants were successfully expressed in the H1299 RB-/- model while exhibiting distinct expression and localization patterns. Among the variants analyzed, HApR552* consistently displayed reduced protein expression together with an altered nucleo-cytoplasmic localization, suggesting that this variant could have a greater impact on RB function and therefore warranted further functional characterization.

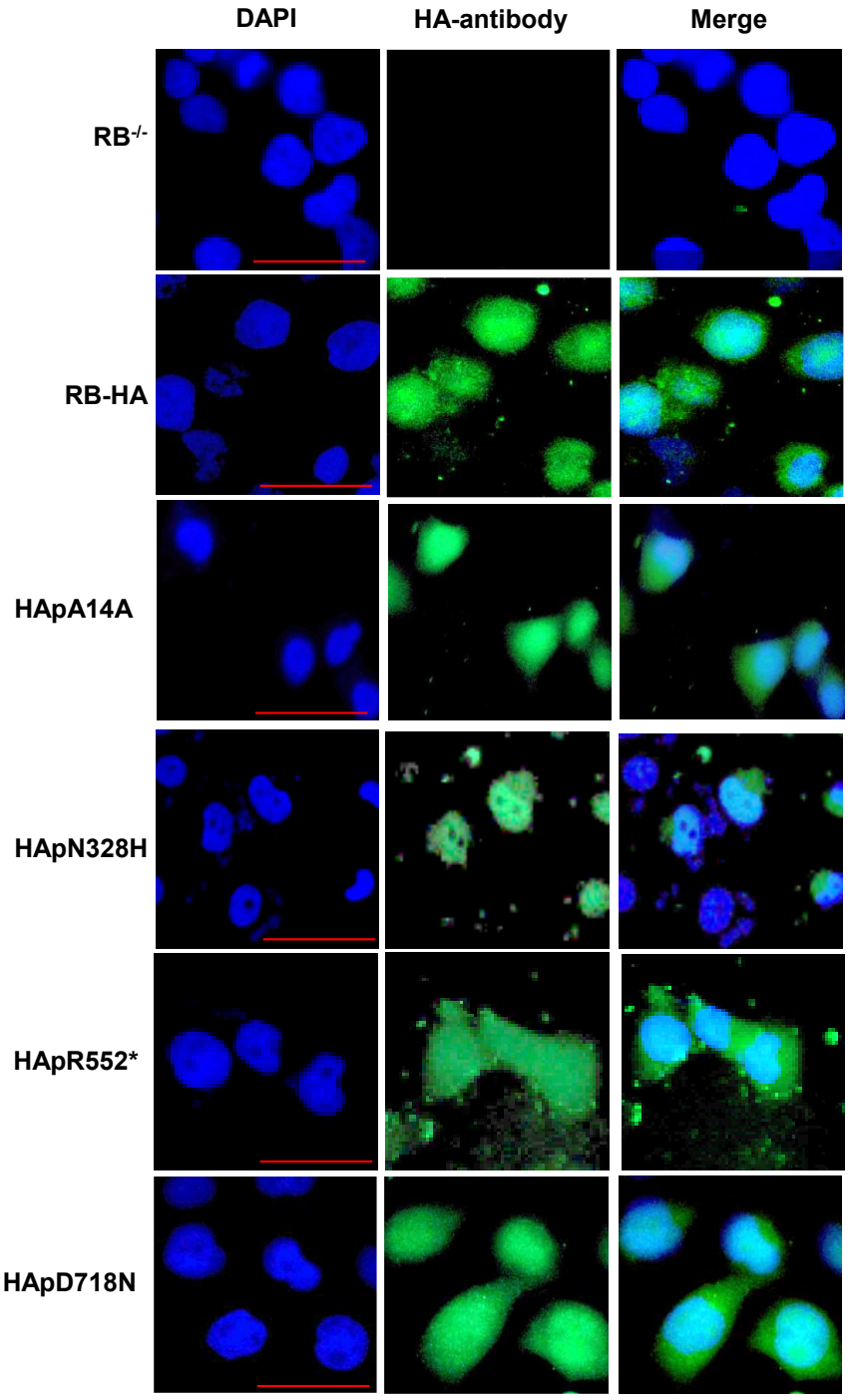

Figure 13. HApA14A, HApR552*, and HApD718N exhibit altered localization.
Immunofluorescence analysis shows that RB-HA and HApN328H are predominantly localized in the nucleus, whereas HApA14A, HApR552*, and HApD718N are detected in both the nuclear and cytoplasmic compartments. HA-tagged RB proteins are shown in green, and nuclei were counterstained with DAPI (blue). Scale bar = 50 μm.

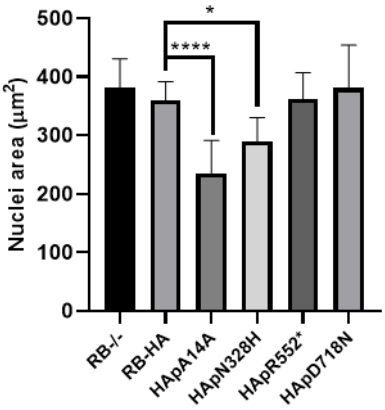

Figure 14. Cells expressing HApA14A or HApN328H exhibit reduced nuclear area.
Nuclear area was quantified from DAPI-stained immunofluorescence images and is presented in µm^2. Cells expressing HApA14A or HApN328H exhibited a significant reduction in nuclear area compared with RB-HA-expressing cells, whereas cells expressing HApR552* or HApD718N showed no significant differences. Results are expressed as mean ± SD. Statistical significance was determined using Student's *t*-test (*p*<0.05, **p<0.0001).
RB

3.3 Cell proliferation, migration, and viability

To determine whether the RB variants affected cellular behavior, we first evaluated cell proliferation using the MTT assay. Four of the variants exhibit higher proliferative activity than RB-HA-expressing cells, with the HApA14A, HApD718N, and truncated HApR552* variants showing the most pronounced increase (Figure 15a). These findings were further supported by direct cell counting over four consecutive days. In agreement with the MTT results, HApA14A and HApR552* displayed the highest proliferation rates, reaching cell numbers more than twice those observed in RB-HA cultures by the end of the experiment. HApD718N also showed enhanced proliferation, whereas HApN328H exhibited only a modest increase relative to RB-HA (Figure 15b).

To further assess the impact of these variants on long-term proliferative capacity, clonogenic assays were performed. Although all cell lines retained the ability to form colonies, consistent with the tumorigenic nature of H1299 cells, only the HApR552* variant exhibited a significant increase in colony formation compared with RB-HA (Figure 16). This result indicates that the truncated variant possesses an enhanced clonogenic potential beyond the increase in short-term proliferation observed in the other variants.

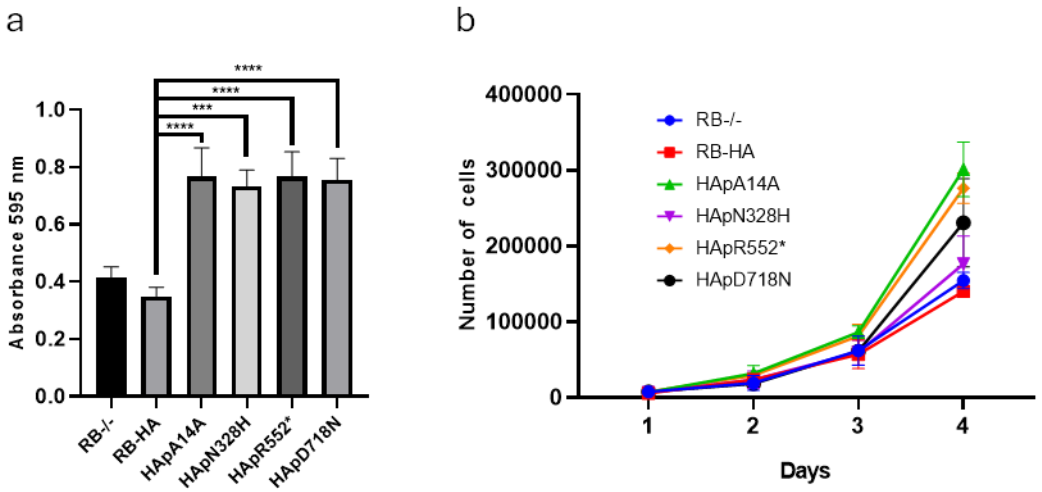

Figure 15. *RB1* variants increase the proliferative activity of H1299 RB-/- cells.
a) The MTT assay shows significantly higher metabolic activity in cells expressing each *RB1* variant than in RB-HA expressing cells, with HApA14A, HApD718N, and HApR552* showing the greatest increases. b) Direct cell counting over four consecutive days shows the highest proliferation rates in cells expressing HApA14A and HApR552*, whereas HApN328H produced only a modest increase relative to RB-HA. Results are expressed as mean ± SD. Statistical significance was determined by one-way ANOVA followed by Bonferroni's multiple-comparison test (*p<0.05, **p<0.01, **p<0.001, ****p<0.0001).

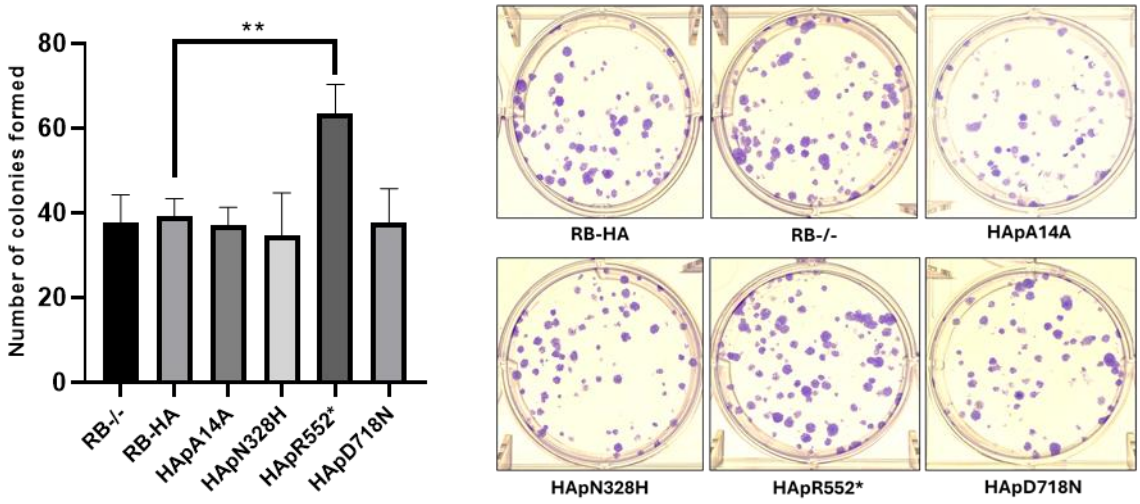

Figure 16. HApR552* exhibits increased clonogenic capacity.
Representative images and quantification of colonies formed by H1299 RB-/- cells expressing the indicated *RB1* variants are shown. Among the variants analyzed, only HApR552* produced a significant increase in colony formation compared with RB-HA. Results are expressed as mean ± SD. Statistical significance was determined by one-way ANOVA followed by Bonferroni's multiple comparisons test (**p<0.01).

Finally, the migratory capacity of each cell line was evaluated using a wound healing assay. Among all RB variants, HApR552* exhibited the highest migration rate, resulting in a markedly greater wound closure than RB-HA and the remaining variants after 48 hours (Figures 17 and 18). These findings demonstrate that, in addition to promoting cell proliferation and clonogenicity, the HApR552* variant also enhances the migratory behavior of H1299 cells.

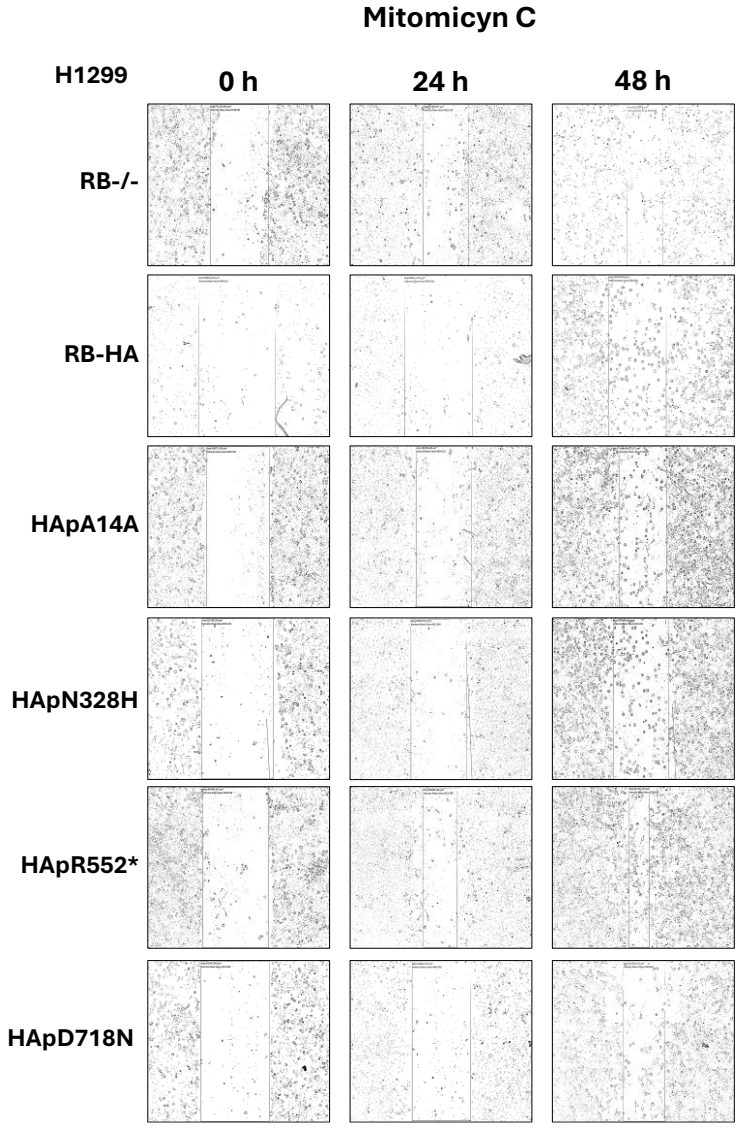

Figure 17. HApR552* exhibits the greatest wound closure among the *RB1* variants.
Representative images of the wound healing assay performed in H1299 RB-/- cells expressing the indicated *RB1* variants are shown at 0, 24, and 48 h after scratch generation. Cells were treated with mitomycin C before wounding to inhibit proliferation. Wound closure was monitored over time, and the migrated area was quantified using ZEN Lite 2012 software.

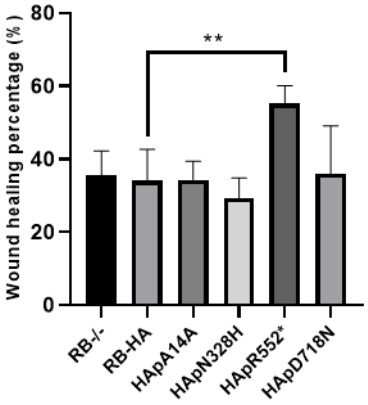

Figure 18. HApR552* exhibits increased migratory capacity.
The graph shows the percentage of wound closure for each cell line. HApR552* exhibited a significantly higher percentage of wound closure than the RB-HA control. Results are expressed as mean ± SD. Statistical significance was determined by one-way ANOVA followed by Bonferroni's multiple comparisons test (*p<0.05, **p<0.01).

3.4 The cellular phenotype associated with R552* is independent of the HA tag.

Since HApR552* consistently exhibits the most pronounced phenotype among the *RB1* variants, we next investigated whether these effects were influenced by the presence of the HA tag. To address this question, a stable H1299 RB-/- cell line expressing the truncated R552* variant without the HA tag (pR552*) was generated and subsequently evaluated using the same functional assays.

Proliferative activity was first assessed using the MTT assay. Cells expressing pR552* exhibit significantly higher proliferative activity than RB-HA-expressing cells, reproducing the phenotype previously observed with HA-tagged HApR552* (Figure 19). Colony-forming capacity was then examined using a clonogenic assay. Consistent with the MTT results, cells expressing pR552* formed significantly more colonies than RB-HA-expressing cells, showing that the increased clonogenic capacity associated with R552* was maintained in the absence of the HA tag (Figure 20).

Finally, to determine whether the HA tag influenced the migratory phenotype associated with R552*, cell migration was evaluated using a wound healing assay. Cells expressing pR552* exhibit significantly greater wound closure than RB-HA expressing cells,

reproducing the increased migratory capacity previously observed in cells expressing HA-tagged HApR552* (Figure 21).

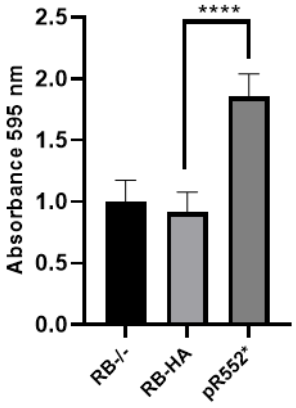

Figure 19. pR552* reproduces the increased proliferative activity observed with HApR552*.
The MTT assay shows that cells expressing pR552* exhibit significantly higher proliferative activity than RB-HA-expressing cells, reproducing the phenotype previously observed with HA-tagged HApR552*. Results are expressed as mean ± SD. Statistical significance was determined by one-way ANOVA followed by Bonferroni's multiple-comparisons test (***p<0.0001).

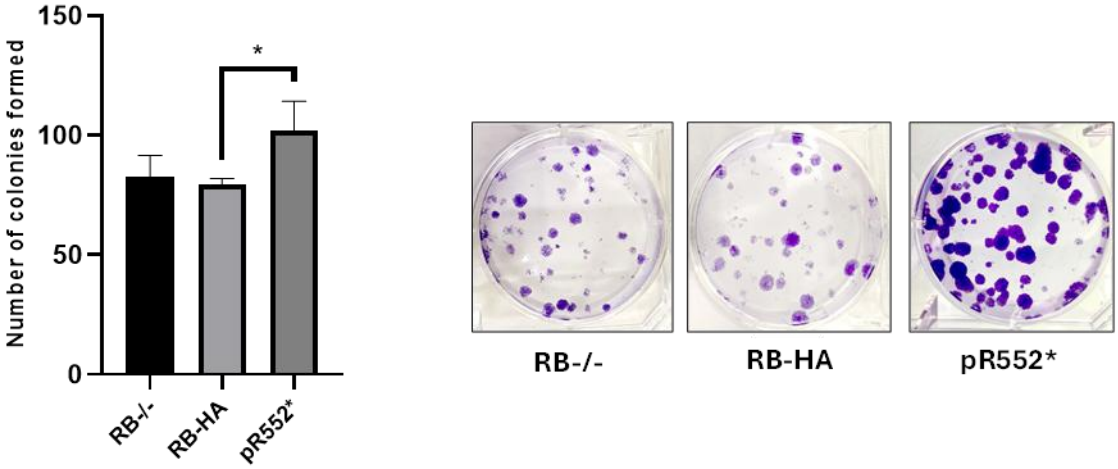

Figure 20. pR552* retains enhanced clonogenic capacity.
Representative images and quantification of the clonogenic assay show that cells expressing untagged pR552* form significantly more colonies than RB-HA-expressing cells. Results are expressed as mean ± SD. Statistical significance was determined using Student's *t*-test (*p<0.05).

Together, these findings demonstrate that the biological effects associated with the truncated mutant are independent of the HA tag and can therefore be attributed to the R552* mutation itself.

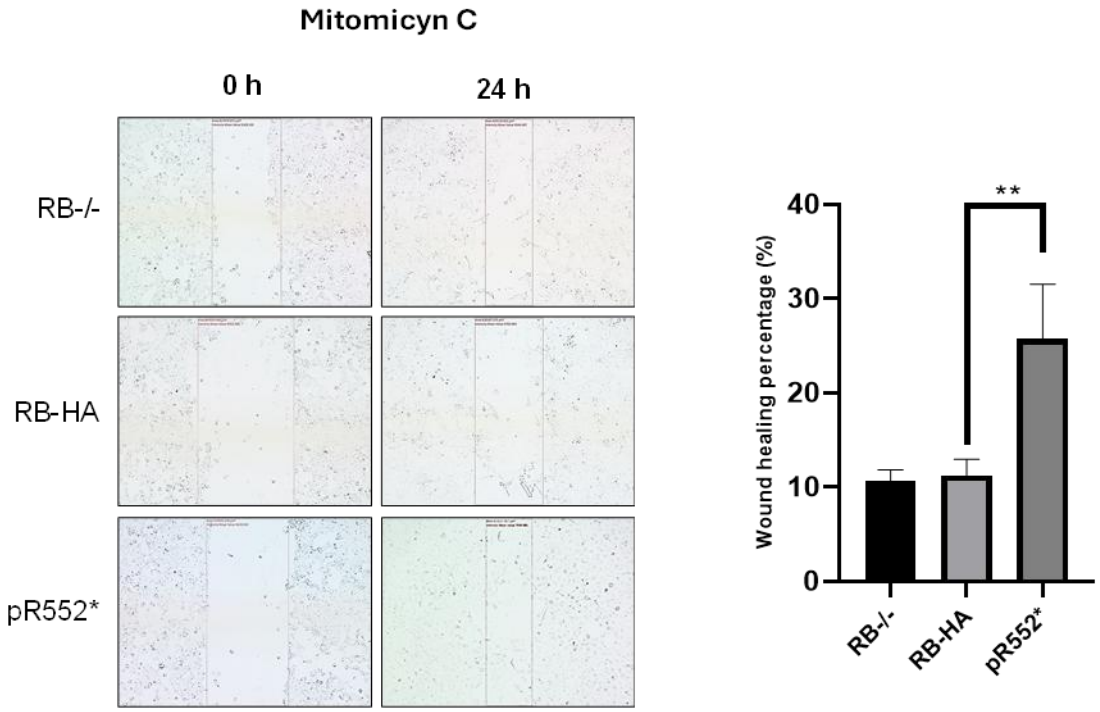

Figure 21. The R552*-associated migratory phenotype persists without HA tagging. Representative images of the wound healing assay are shown in the left panel. Quantification of wound closure in the right panel shows that cells expressing pR552* reach a significantly higher percentage of wound closure than RB-HA-expressing cells. Results are expressed as mean ± SD. Statistical significance was determined using Student's *t*-test (*p<0.01)

3.5 The pR552* variant exhibits a gain-of-function phenotype

We next investigated whether the phenotype associated with HApR552* persisted when the variant was co-expressed with wild-type RB or whether the wild-type protein could restore normal cellular behavior. H1299 RB-/- cells were therefore co-transfected with HApR552* and RB-HA, and their migratory capacity was evaluated using a wound healing assay. Cells were treated with mitomycin C before scratch generation to inhibit cell proliferation. Cells co-expressing HApR552* and RB-HA displayed a wound closure percentage comparable to that observed in cells expressing RB-HA, indicating that the presence of the wild-type protein did not reverse the enhanced migratory phenotype associated with HApR552* (Figure 22).

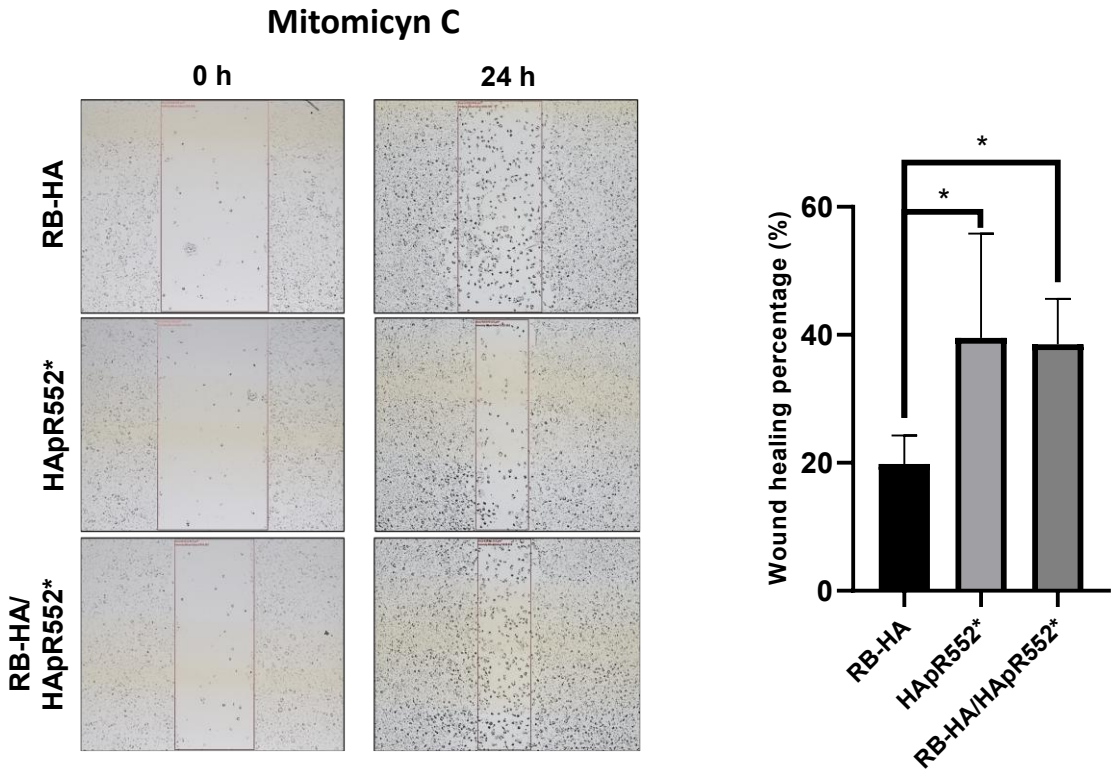

Figure 22. The increased migratory capacity associated with HApR552* persists in the presence of wild-type RB.
Representative images of the wound healing assay performed in H1299 RB-/- cells expressing RB-HA, HApR552*, or both constructs are shown at 0 and 24 h after scratch generation (left panel). Quantification of wound closure (right panel) shows that cells co-expressing RB-HA and HApR552* retain the elevated migratory capacity observed in cells expressing HApR552* alone. Results are expressed as mean ± SD. Statistical significance was determined by one-way ANOVA (*p<0.05).

We subsequently evaluated the subcellular localization pattern resulting from the co-expression of wild-type RB and the R552* variant. To distinguish the proteins independently, we used two different tags: wild-type RB was tagged with Flag, while R552* retained the HA tag. Thus, using immunofluorescence, we were able to detect RB-Flag in green and HApR552* in red. RB-Flag maintained its predominantly nuclear localization, whereas HApR552* was detected in both the nucleus and the cytoplasm. This nucleo-cytoplasmic distribution of HApR552* persisted in the co-transfected cells, demonstrating that the presence of wild-type RB was insufficient to restore the nuclear localization of the truncated variant (Figure 23). Together with the wound healing results, these findings support the gain-of-function behavior of HApR552*.

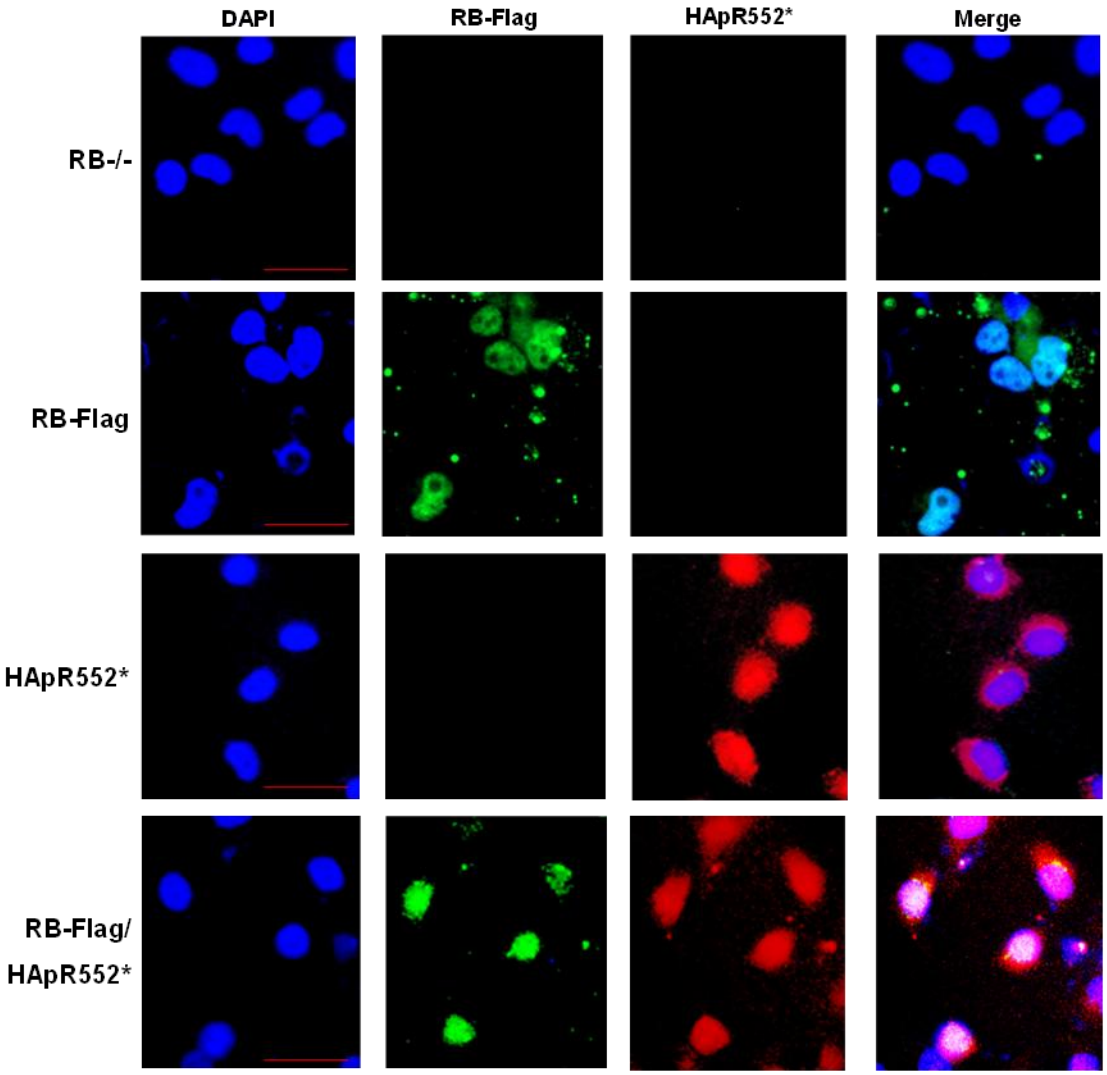

Figure 23. HApR552* retains its nucleo-cytoplasmic localization in the presence of wild-type RB.

H1299 RB-/- cells were co-transfected with RB-Flag and HApR552* to visualize the two proteins independently by immunofluorescence. RB-Flag (green) remained predominantly localized in the nucleus, whereas HApR552* (red) was detected in both the nuclear and cytoplasmic compartments. The persistence of this distribution in co-transfected cells shows that wild-type RB is insufficient to restore the nuclear localization of the truncated variant. Nuclei were counterstained with DAPI (blue). Scale bar = 50 μm.

4 Discussion

This study examined the cellular consequences of four *RB1* variants identified in patients with retinoblastoma: A14A, N328H, R552* and D718N. Their characterization in an H1299 RB-/- background revealed that the variants were not functionally equivalent, despite all being expressed at the transcript and protein levels. Differences in protein abundance and subcellular localization were accompanied by distinct effects on cell proliferation, clonogenic capacity, and migration. Among the variants analyzed, R552* produced the most consistent and pronounced cellular phenotype, characterized by altered nucleo-cytoplasmic localization and increased proliferative, clonogenic, and migratory capacities. These findings demonstrate that *RB1* variants associated with retinoblastoma can affect RB behavior through different cellular mechanics and identify R552* as the variant with the greatest functional impact in this experimental model.

The expression results demonstrate that all *RB1* variants were successfully expressed in H1299 RB-/- cells at both the transcript and protein levels, although differences in transcript abundance were observed among the constructs. Importantly, the lack of detection of the N328H and R552* variants with the anti-RB antibody did not reflect an absence of protein expression, as both proteins were readily detected using the HA tag. Furthermore, the lower apparent molecular weight of the R552* variant was consistent with the predicted truncated protein generated by the premature stop codon. Collectively, these findings validate the expression of *RB1* variants and provide a solid foundation for subsequent functional studies.

The localization results provide additional evidence that protein abundance alone does not determine the behavior of the *RB1* variants. D718N reached protein levels comparable to wild-type RB but displayed a nucleo-cytoplasmic distribution, suggesting that the substitution may interfere with protein folding, molecular interactions, nuclear transport, or nuclear retention[32–37]. A14A also exhibits a nucleo-cytoplasmic distribution, raising the possibility that changes in translation kinetics could influence protein folding and

localization without changing its amino acid sequence. In contrast, N328H remained predominantly nuclear, but cells expressing N328H showed a significant reduction in nuclear area. A similar reduction was observed in cells expressing A14A. Rb participates in cell cycle regulation and the organization of chromosomal regions[53]. These morphological changes could reflect alterations in cell cycle state, chromatin organization, or nuclear architecture. Nevertheless, nuclear area alone cannot identify the underlying mechanism, and additional analysis would be required to determine its biological significance.

Among variants analyzed, R552* produced the most pronounced and consistent functional alterations. The premature stop at residue 552 generates a truncated RB protein that lacks a substantial portion of the pocket domain, the complete C-terminal region, and the nuclear localization signal required for efficient transport of RB into the nucleus. These regions are also necessary for interactions with E2F and other regulatory proteins and for the transcriptional repressor activity of RB[32–37]. Their absence therefore provides a plausible explanation for the nucleo-cytoplasmic localization of HApR552* and its inability to reproduce the growth suppressive behavior of wild-type RB. Disruption of the RB-E2F interaction could allow continued expression of genes required for cell cycle progression, contributing to the increased proliferative activity observed in cells expressing this variant[31,42,51]. However, R552* was also associated with enhanced clonogenic capacity and highest migratory activity among the variants, suggesting that its cellular effects may extend beyond impaired cell cycle control. The presence of these phenotypes despite the relatively low abundance of the truncated protein further suggests that R552* is not simply an unstable or inactive product. Nevertheless, additional experiments examining E2F activity, interaction partners, protein stability, and downstream transcriptional changes would be required to establish the molecular mechanisms responsible for its behavior.

Because the initial characterization of R552* was performed using an HA-tagged construct, it was necessary to determine whether the epitope tag contributes to the observed cellular effects. This possibility was particularly relevant because the addition of a tag could potentially alter the stability, interactions, or behavior of a truncated protein. The untagged pR552* construct reproduced the increased proliferative, clonogenic, and migratory

capacities previously observed with HApR552*. The consistency of these phenotypes across the tagged and untagged constructs indicates that they are associated with the R552* alteration rather than being an artifact caused by the HA tag. This control therefore strengthens the interpretation that the truncated RB protein possesses intrinsic properties that modify cellular behavior.

Having established that the functional phenotype of R552* was independent of the HA tag, we next considered whether wild-type RB could suppress the effects associated with the variant. According to Knudson's two-hit hypothesis, retinoblastoma development generally requires the functional inactivation of both *RB1* alleles[14]. In the present study, however, coexpression of wild-type RB did not reduce the enhanced migratory capacity associated with HApR552*. Immunofluorescent analysis also showed that the variant retained its nucleo-cytoplasmic distribution in cells that simultaneously expressed nuclear wild-type RB. These findings indicate that wild-type RB was insufficient to reverse the localization and migratory phenotypes produced by HApR552* under the experimental conditions examined. This persistence suggests that R552* may exert a dominant cellular effect rather than behaving exclusively as a conventional recessive loss-of-function (LOF) variant.

Taken together, the persistence of the R552* associated phenotypes in the presence of wild-type RB is compatible with a potential gain-of-function (GOF) like behavior. A conventional LOF variant would primarily be expected to reduce or eliminate the normal tumor-suppressive activity of RB, whereas a GOF variant would acquire an additional activity that actively modifies cellular behavior[54]. GOF mechanisms have been extensively described for other tumor suppressors, particularly p53, whose altered forms can promote proliferation, survival, migration, and genomic instability through activities that are distinct from the loss of wild-type p53 function[11,55–58]. In the case of R552*, the increased proliferation, clonogenic capacity, and migration, together with the persistence of its localization and migratory phenotypes during co-expression with wild-type RB, support the possibility that the truncated protein exerts effects beyond the simple absence of functional RB. However, these findings do not yet establish the molecular mechanisms underlying these

phenotypes. The altered subcellular localization of the R552* protein further suggests the existence of novel functional interactions, but additional studies will be required to identify its molecular targets and determine whether R552* represents a genuine GOF *RB1* variant.

The interpretation of these findings should consider the experimental context in which the *RB1* variants were evaluated. CRISPR/Cas9-mediated disruption of *RB1* provided a common RB-deficient background, while retroviral transduction allowed sustained expression of corresponding constructs throughout the experiments. However, exogenous expression does not fully recapitulate endogenous allelic regulation or the expression levels expected in a heterozygous cell. In addition, H1299 is a p53-deficient non-small cell lung cancer cell line whose cellular context differs substantially from that of the developing retina. Therefore, future validation in other models will be important to determine the physiological relevance of these findings. Complementary mechanistic studies addressing E2F activity, protein stability, nuclear transport, protein interactions, and downstream transcriptional programs will also be necessary to define the molecular basis of the phenotypes associated with R552*.

5 Conclusions

This study provides a functional characterization of four *RB1* variants associated with retinoblastoma (A14A, N328H, R552*, and D718N) using an RB-deficient H1299 cellular model. Although all variants were expressed, they exhibited distinct patterns of RNA and protein abundance, subcellular localization, and cellular behavior, demonstrating that *RB1* variants have distinct functional consequences and may alter RB biology through different mechanisms.

Among the variants analyzed, R552* consistently displayed the most pronounced phenotype. The truncated protein exhibits altered nucleo-cytoplasmic localization together with increased proliferation, clonogenic capacity, and migratory activity, suggesting that its effects extend beyond those expected from a simple loss of RB tumor suppressive function. The persistence of key phenotypes during co-expression with wild-type RB further supports the hypothesis that R552* may exert a dominant cellular effect compatible with a potential GOF-like behavior.

While the altered subcellular localization of the R552* protein may reflect altered protein interactions, additional studies will be required to identify its molecular targets and determine whether it represents a genuine GOF *RB1* variant. Validation in physiologically relevant retinal models will also be necessary to confirm the biological significance of these findings.

Overall, this work expands the functional characterization of *RB1* variants associated with retinoblastoma and identifies R552* as a high-priority candidate for future mechanistic studies. These findings contribute to a better understanding of the distinct functional consequences of *RB1* variants and provide a foundation for investigating how specific *RB1* alterations may influence retinoblastoma biology.

6 References

1. Malacinski, G. M. Mutations, Mutagenesis, and DNA Repair. in *Essentials of Molecular Biology* 491 (Jones and Bartlett Publishers, 2003).

2. Mahmood, A., Jalal, S., Shabbir, M. U. & Sharma, S. Biochemistry, Mutation. in *StatPearls* (StatPearls Publishing, 2024).

3. László, P. Mutations. in *Protein Evolution* 228–240 (Blackwell Science, Oxford, 1999).

4. Sharma, Y. *et al.* A pan-cancer analysis of synonymous mutations. *Nat. Commun.* **10**, (2019).

5. Diederichs, S. *et al.* The dark matter of the cancer genome: aberrations in regulatory elements, untranslated regions, splice sites, non-coding RNA and synonymous mutations . *EMBO Mol. Med.* **8**, 442–457 (2016).

6. Supek, F., Miñana, B., Valcárcel, J., Gabaldón, T. & Lehner, B. Synonymous mutations frequently act as driver mutations in human cancers. *Cell* **156**, 1324–1335 (2014).

7. Wu, K., Qin, D., Qian, Y. & Liu, H. A new era of mutation rate analyses : Concepts and methods. **45**, 767–780 (2024).

8. Mort, M., Ivanov, D., Cooper, D. N. & Ã, N. A. C. A Meta-Analysis of Nonsense Mutations Causing Human Genetic Disease. **29**, 1037–1047 (2008).

9. Stalder, L. & Mühlemann, O. The meaning of nonsense. *Trends Cell Biol.* **18**, 315–321 (2008).

10. Benhabiles, H., Jia, J. & Lejeune, F. Pathologies Susceptible to be Targeted for Nonsense Mutation Therapies. *Nonsense Mutat. Correct. Hum. Dis.* 77–105 (2016) doi:10.1016/b978-0-12-804468-1.00002-6.

11. Song, H., Hollstein, M. & Xu, Y. p53 gain-of-function cancer mutants induce genetic instability by inactivating ATM. **9**, (2007).

12. Sehn, J. K. Insertions and Deletions (Indels). 129–150 (2015) doi:10.1016/B978-0-12-404748-8.00009-5.

13. Institute, N. H. G. R. Pathogenic Variant. https://www.genome.gov/genetics-glossary/Pathogenic-Variant (2023).

14. Knudson, A. G. Mutation and cancer: statistical study of retinoblastoma. *Proc. Natl. Acad. Sci. U. S. A.* (1971) doi:10.1073/pnas.68.4.820.

15. Sherr, C. J. Principles of Tumor Suppression. *Cell* **116**, 235–246 (2004).

16. Xu, X. L. *et al.* Rb suppresses human cone-precursor-derived retinoblastoma tumours. *Nature* (2014) doi:10.1038/nature13813.

17. Robert Cronin Yung Peng, Rose Khavari, N. D. Retinoblastoma. *Physiol. Behav.* **176**,

139–148 (2017).

18. Dimaras, H., Corson, T. W., Cobrinik, D., White, A. & Zhao, J. Retinoblastoma. (2015) doi:10.1038/nrdp.2015.21.

19. Lansingh, V. C. *et al.* Retinoblastoma in Mexico: Part I. A review of general knowledge of the disease, diagnosis, and management. *Boletin Medico del Hospital Infantil de Mexico* (2015) doi:10.1016/j.bmhimx.2015.09.001.

20. Canturk, S. *et al.* Survival of retinoblastoma in less-developed countries impact of socioeconomic and health-related indicators. *Br. J. Ophthalmol.* (2010) doi:10.1136/bjo.2009.168062.

21. Leal-Leal, C. *et al.* A multicentre report from the Mexican Retinoblastoma Group. *Br. J. Ophthalmol.* (2004) doi:10.1136/bjo.2003.035642.

22. Ramírez-ortiz, M. A. *et al.* Systematic review of the current status of programs and general knowledge of diagnosis and management of retinoblastoma. **74**, (2017).

23. Pandey, A. N. Retinoblastoma: An overview. *Saudi Journal of Ophthalmology* (2014) doi:10.1016/j.sjopt.2013.11.001.

24. Murphree, A. L. Intraocular Retinoblastoma : the Case for a New Group Classification. **18**, 41–53 (2005).

25. Fabian, I. D., Reddy, A. & Sagoo, M. S. Classification and staging of retinoblastoma. *Community Eye Heal. J.* 3 (2018).

26. Fabian, I. D. *et al.* The management of retinoblastoma. *Oncogene* (2018) doi:10.1038/s41388-017-0050-x.

27. Mendoza, P. R. & Grossniklaus, H. E. *The Biology of Retinoblastoma*. *Progress in Molecular Biology and Translational Science* vol. 134 (Elsevier Inc., 2015).

28. Machín, E. *et al.* Retinoblastoma: A molecular, clinical and therapeutic approach. *Arch. Venez. Farmacol. y Ter.* (2017).

29. Grossniklaus, H. E. Retinoblastoma. Fifty years of progress. the LXXI Edward Jackson memorial lecture. *Am. J. Ophthalmol.* (2014) doi:10.1016/j.ajo.2014.07.025.

30. Rodriguez-Galindo, C., Orbach, D. B. & VanderVeen, D. Retinoblastoma. *Pediatric Clinics of North America* (2015) doi:10.1016/j.pcl.2014.09.014.

31. Giacinti, C. & Giordano, A. RB and cell cycle progression. *Oncogene* (2006) doi:10.1038/sj.onc.1209615.

32. Chow, K. N. & Dean, D. C. Domains A and B in the Rb pocket interact to form a transcriptional repressor motif. *Mol. Cell. Biol.* (1996) doi:10.1128/mcb.16.9.4862.

33. Qin, X. Q., Chittenden, T., Livingston, D. M. & Kaelin, W. G. Identification of a growth suppression domain within the retinoblastoma gene product. *Genes Dev.* (1992) doi:10.1101/gad.6.6.953.

34. Sellers, W. R., Rodgers, J. W. & Kaelin, W. G. A potent transrepression domain in the

retinoblastoma protein induces a cell cycle arrest when bound to E2F sites. *Proc. Natl. Acad. Sci. U. S. A.* (1995) doi:10.1073/pnas.92.25.11544.

35. Hassler, M. *et al.* Crystal Structure of the Retinoblastoma Protein N Domain Provides Insight into Tumor Suppression, Ligand Interaction, and Holoprotein Architecture. *Mol. Cell* (2007) doi:10.1016/j.molcel.2007.08.023.

36. Lee, J. O., Russo, A. A. & Pavletich, N. P. Structure of the retinoblastoma tumour-suppressor pocket domain bound to a peptide from HPV E7. *Nature* (1998) doi:10.1038/36038.

37. Rubin, S. M., Gall, A. L., Zheng, N. & Pavletich, N. P. Structure of the Rb C-terminal domain bound to E2F1-DP1: A mechanism for phosphorylation-induced E2F release. *Cell* (2005) doi:10.1016/j.cell.2005.09.044.

38. DeCaprio, J. A. *et al.* SV40 large tumor antigen forms a specific complex with the product of the retinoblastoma susceptibility gene. *Cell* (1988) doi:10.1016/0092-8674(88)90559-4.

39. Dyson, N. *et al.* Large T antigens of many polyomaviruses are able to form complexes with the retinoblastoma protein. *J. Virol.* (1990) doi:10.1128/jvi.64.3.1353-1356.1990.

40. Whyte, P., Williamson, N. M. & Harlow, E. Cellular targets for transformation by the adenovirus E1A proteins. *Cell* (1989) doi:10.1016/0092-8674(89)90984-7.

41. Nicholas Dyson, Peter M. Howley, Karl Monger, E. H. The Human Papilloma Virus-16 E7 Oncoprotein Is Able to Bind to the Retinoblastoma Gene Product. *Science (80-.).* (1989).

42. Weinberg, R. A. The retinoblastoma protein and cell cycle control. *Cell* (1995) doi:10.1016/0092-8674(95)90385-2.

43. De Falco, G., Comes, F. & Simone, C. pRb: Master of differentiation. Coupling irreversible cell cycle withdrawal with induction of muscle-specific transcription. *Oncogene* (2006) doi:10.1038/sj.onc.1209623.

44. Khidr, L. & Chen, P. L. RB, the conductor that orchestrates life, death and differentiation. *Oncogene* (2006) doi:10.1038/sj.onc.1209612.

45. Chau, B. N. & Wang, J. Y. J. Coordinated regulation of life and death by RB. *Nature Reviews Cancer* (2003) doi:10.1038/nrc993.

46. Skapek, S. X., Pan, Y. R. & Lee, E. Y. H. P. Regulation of cell lineage specification by the retinoblastoma tumor suppressor. *Oncogene* (2006) doi:10.1038/sj.onc.1209710.

47. Stengel, K. R. *et al.* RB/p107/130 pocket proteins: Protein dynamics and interactions with target gene promoters. *J. Biol. Chem.* (2009).

48. Ying, H. & Xiao, Z. X. J. Targeting retinoblastoma protein for degradation by proteasomes. *Cell Cycle* (2006) doi:10.4161/cc.5.5.2515.

49. Sdek, P. *et al.* MDM2 promotes proteasome-dependent ubiquitin-independent degradation of retinoblastoma protein. *Mol. Cell* (2005) doi:10.1016/j.molcel.2005.10.017.

50. Higashitsuji, H., Liu, Y., Mayer, R. J. & Fujita, J. The oncoprotein gankyrin negatively regulates both p53 and RB by enhancing proteasomal degradation. *Cell Cycle* (2005) doi:10.4161/cc.4.10.2107.

51. Dyson, N. J. RB1: A prototype tumor suppressor and an enigma. *Genes Dev.* **30**, 1492–1502 (2016).

52. COSMIC. https://cancer.sanger.ac.uk/cosmic/.

53. Krishnan, B. *et al.* Active RB causes visible changes in nuclear organization. *J. Cell Biol.* **221**, doi:10.1083/jcb.202102144. (2022).

54. Fay, D. & Biology, M. Genetic mapping and manipulation : Chapter 8-Dominant mutations *. 1–6 (2006) doi:10.1895/wormbook.1.97.1.

55. Matas, D. *et al.* Integrity of the N-terminal transcription domain of p53 is required for mutant p53 interference with drug-induced apoptosis. **20**, 4163–4172 (2001).

56. Sigal, A., Matas, D., Almog, N., Gold, N. & Rotter, V. The C-terminus of mutant p53 is necessary for its ability to interfere with growth arrest or apoptosis. **135**, (2001).

57. Ortiz, E. A. *et al.* Mutant p53 gain - of - function stimulates canonical Wnt signaling via PI3K / AKT pathway in colon cancer. *J. Cell Commun. Signal.* **17**, 1389–1403 (2023).

58. Olivares-Illana, V. & Fåhraeus, R. P53 isoforms gain functions. *Oncogene* **29**, 5113–5119 (2010).

7 Published Article

Analysis of pathogenic variants in retinoblastoma reveals a potential gain-of-function mutation.

Ana María Peña-Balderas, Mayra Martínez-Sánchez, Isaí Olmos-Sánchez, Karla Calderón-González, Mariana Moctezuma-Dávila, Matha Rangel-Charqueño, Jesús Hernández-Monge and Vanesa Olivares-Illana.

Genes & Cancer. 239, 16:1-15. (2025)